

CORRELATIONS AND MULTIPLICITY DISTRIBUTIONS IN MULTIPARTICLE PRODUCTION

BY M. LE BELLAC

University of Nice*

(Presented at the XIII Cracow School of Theoretical Physics, Zakopane, June 1-12, 1973)

A general discussion of Short Range Order hypothesis and its comparison with experimental data on correlations in inclusive spectra is given.

1. Introduction

In the absence of a theory of strong interactions, one of the main purposes of the present experiments on multiparticle production is to discover empirical regularities in the experimental data, in the hope that these regularities will be useful later for a more fundamental understanding of hadrodynamics. Some of these empirical regularities have already been known for many years, from cosmic ray experiments, and have been confirmed later by accelerators. The following regularities are well-known:

Transverse momenta are strongly damped and the average value $\overline{p_T}$ of p_T is of order 350 MeV.

There is a leading particle effect, and the leading particles take off about half of the available energy in the collision.

The average multiplicity grows much slower than what would be allowed by energy-momentum conservation: the growth of the charged multiplicity \bar{n}_c is fairly well approximated by $\bar{n}_c \cong 2 \ln(s/m_p^2) - 4$, where m_p is the proton mass.

In the past two years, another very important property of multiparticle production has been confirmed by experimental data: the one-particle inclusive spectra have been shown to satisfy the scaling behaviour conjectured by Wilson [1] more than ten years ago, and more recently by Feynman [2], and Yang *et al.* [3]. A very attractive way of understanding the scaling behaviour of one particle inclusive distributions is to assume that multiparticle production obeys what may be called short range order (SRO). This concept will be discussed in detail in Section 3; let me only say now that it means lack of correlations between particles with very different rapidities.

* Address: Lab. de Physique Théorique, Faculté des Sciences, Parc Valrose, Nice, France.

However, this SRO hypothesis is only one possible way of deriving the scaling behaviour of one particle inclusive distributions. It is well known for example that the so-called fragmentation models [4] may also be compatible with scaling. In order to test the SRO hypothesis in an unambiguous way, it is necessary to measure inclusive two-particle distributions, from which one can compute correlations. The main purpose of these lectures is to discuss the SRO hypothesis, and to compare its predictions with the present experimental data. I shall show that the present data are fully compatible with SRO, and it is likely that this property will have to be added to the previously well established properties of multiparticle production.

The plan of these lectures is as follows: in Section 2, I collect some useful definitions and kinematical results. In Section 3 I discuss in detail the SRO hypothesis and its consequences, and I make the comparison with experimental data on correlations in Section 4. Section 5 is devoted to an analysis of multiplicity distributions, based on SRO, and finally in Section 6 I examine the correlations between charged and neutral particles.

2. Basic definitions and kinematical results

In this Section I give some useful definitions and kinematical results; in order to come as soon as possible to the discussion of experimental data, I shall omit most of the proofs, which can be found for example in Ref. [4] and references quoted therein.

Kinematical variables

If a secondary is produced with longitudinal momentum p_L and transverse momentum p_T , one can define the usual Feynman variable x and the rapidity y by:

$$p_L = \frac{1}{2}x\sqrt{s}, \quad (2.1)$$

$$p_L = \sqrt{p_T^2 + m^2} \sinh y = m_T \sinh y. \quad (2.2)$$

Let me recall that the basic virtue of the rapidity y is its simple transformation law under a longitudinal boost φ :

$$y \rightarrow y' = y - \varphi.$$

Then, because of Lorentz invariance along the z -axis, any physical quantity can be only a function of rapidity differences. In a high energy reaction $a+b \rightarrow c + \dots$, the rapidities of particles a and b in the center-of-mass system are given by:

$$y_a \simeq \frac{1}{2} \ln \frac{s}{m_a^2}, \quad y_b \simeq -\frac{1}{2} \ln \frac{s}{m_b^2}. \quad (2.3)$$

The difference $Y = y_a - y_b$, which is Lorentz invariant, is the length of the rapidity plot and its value is given by:

$$Y = y_a - y_b = \ln (s/m_a m_b). \quad (2.4)$$

The rapidity of a secondary c will be limited in absolute value:

$$|y_c| \leq \frac{1}{2} \ln \left(\frac{s}{m_c^2} \right) = \frac{1}{2} \left| Y + \ln \left(\frac{m_a m_b}{m_c^2} \right) \right|. \quad (2.5)$$

In practice the most important case is that of a proton-proton collision, the produced particle c being a pion; (2.5) becomes:

$$|y_\pi| \leq \frac{1}{2} Y + \ln \left(\frac{m_p}{m_\pi} \right) \simeq \frac{1}{2} Y + 1.9. \quad (2.6)$$

However, the yield of pions having $|y_\pi| > \frac{1}{2} Y$ is small. In order to fix ideas, let me give Y in three typical cases:

E_{lab} (GeV):	25	300	1,500
Y :	4.0	6.5	8.2

Finally, in experiments where only the production angle Θ is measured, there is an approximate relation between Θ and y , valid provided $p_T^2 \gg m^2$:

$$y \simeq -\ln \tan \Theta/2 \equiv \eta. \quad (2.7)$$

Inclusive distributions (case of identical particles)

Let me call $N_1(\mathbf{p}; s)$ the normalized inclusive one particle distribution for the reaction $a+b \rightarrow c(\mathbf{p}) + \text{anything}$:

$$N_1(\mathbf{p}; s) = \frac{1}{\sigma} \frac{d\sigma}{dp}, \quad (2.8)$$

where $dp = d^3p/E$ and I consider for the moment identical particles only. The normalization cross-section is generally chosen to be the total inelastic cross-section but other choices are possible; this problem is important and will be discussed further in Section 5. Similarly one defines the normalized k -particle inclusive distribution for the reaction $a+b \rightarrow c_1(\mathbf{p}_1) + c_2(\mathbf{p}_2) + \dots + c_k(\mathbf{p}_k) + \text{anything}$:

$$N_k(\mathbf{p}_1, \dots, \mathbf{p}_k; s) = \frac{1}{\sigma} \frac{d\sigma}{dp_1 \dots dp_k}. \quad (2.9)$$

The simplest guess for the two-particle distribution N_2 would be to take the product of two one-particle distributions:

$$N_2(\mathbf{p}_1, \mathbf{p}_2; s) = N_1(\mathbf{p}_1; s) N_1(\mathbf{p}_2; s). \quad (2.10)$$

The correlation C_2 will be defined as the difference between the actual two-particle distribution and the guess (2.10):

$$C_2(\mathbf{p}_1, \mathbf{p}_2; s) = N_2(\mathbf{p}_1, \mathbf{p}_2; s) - N_1(\mathbf{p}_1; s) N_1(\mathbf{p}_2; s). \quad (2.11)$$

Similarly the 3-particle correlation will be defined as the difference between N_3 and the "expected" value:

$$\begin{aligned} C_3(\mathbf{p}_1, \mathbf{p}_2, \mathbf{p}_3; s) = & N_3(\mathbf{p}_1, \mathbf{p}_2, \mathbf{p}_3; s) - \\ & - \{N_1(\mathbf{p}_1; s)C_2(\mathbf{p}_2, \mathbf{p}_3; s) + 2 \text{ permutations}\} - \\ & - N_1(\mathbf{p}_1; s) N_1(\mathbf{p}_2; s) N_1(\mathbf{p}_3; s). \end{aligned} \quad (2.12)$$

The general form for C_k can be easily inferred from (2.12).

Relation between integrated correlations and moments of the multiplicity distribution

Let me call $P(n, s)$ the ratio of the partial cross-section $\sigma_n(s)$ for producing n final particles to the total cross-section $\sigma(s)$: $P(n, s) = \sigma_n(s)/\sigma(s)$. Since $\sigma(s) = \sum_n \sigma_n(s)$, $P(n, s)$ is a probability distribution ($P(n; s) \geq 0$ and $\sum_n P(n; s) = 1$), which is usually called the multiplicity distribution (MD), one can define various moments of the MD in the standard way, and important result is that the integral of the k -particle distribution N_k is equal to the factorial moment of order k , which I denote by F_k :

$$\begin{aligned} F_k = & \overline{n(n-1)\dots(n-k+1)} = \\ = & \sum n(n-1)\dots(n-k+1)P(n) \\ = & \int N_k dp_1 \dots dp_k. \end{aligned} \quad (2.13)$$

(I omit the variable s , when it does not play any role.) This relation generalizes the well-known result:

$$\frac{1}{\sigma} \int \frac{d\sigma}{dp} dp = \int N_1 dp = \bar{n}.$$

The integrals of the correlations C_k are often referred to as Mueller's moments [5] and denoted by f_k :

$$f_k = \int C_k dp_1 \dots dp_k. \quad (2.14)$$

From (2.11), (2.12) and (2.13) we immediately derive:

$$\begin{aligned} f_1 = & F_1 = \bar{n}, \\ f_2 = & F_2 - F_1^2 = \overline{n(n-1)} - \bar{n}^2, \\ f_3 = & F_3 - 3F_1F_2 + 2F_1^3 \\ = & \overline{n(n-1)(n-2)} - 3\bar{n}\overline{n(n-1)} + 2\bar{n}^3. \end{aligned} \quad (2.15)$$

Generating functions

In probability theory, it is often convenient to work with generating function; let me for example build the following generating function:

$$G(z) = \sum_n z^n P(n). \quad (2.16)$$

Clearly:

$$\left. \frac{d^k}{dz^k} G(z) \right|_{z=1} = F_k$$

so that:

$$G(z) = \sum_k \frac{(z-1)^k}{k!} F_k. \quad (2.17)$$

Now, a well-known technique in statistical mechanics allows to relate the factorial moments to Mueller's moments [5]; in fact one can prove that

$$G(z) = \exp \left\{ \sum_k \frac{(z-1)^k}{k!} f_k \right\} = \exp \{g(z)\}. \quad (2.18)$$

In order to see the usefulness of $G(z)$, let us assume that all f_k 's, but f_1 , are zero. Then $G(z) = \exp [\bar{n}(z-1)]$ and

$$P(n) = \frac{1}{n!} \left. \frac{d^n G(z)}{dz^n} \right|_{z=0} = \frac{(\bar{n})^n e^{-\bar{n}}}{n!} \quad (2.19)$$

which is the Poisson distribution. This is not surprising: if all the correlations vanished, then we would have $f_k = 0$ for $k \geq 2$ and the Poisson distribution corresponds simply to independent emission of particles. More generally, Mueller's moments f_k measure the departure from a Poisson distribution; in particular $f_2 < 0$ means that the MD is narrower than Poisson, $f_2 > 0$ means that it is broader than Poisson.

Another useful generating function is that corresponding to the usual moments v_k :

$$\begin{cases} v_k = \bar{n}^k = \sum n^k P(n) = \left. \frac{d^k}{dz^k} H(z) \right|_{z=0}, \\ H(z) = \sum e^{zn} P(n). \end{cases} \quad (2.20)$$

To the central moments $\mu_k = \overline{(n-\bar{n})^k}$ corresponds the generating function

$$\tilde{H}(z) = \sum e^{z(n-\bar{n})} P(n) = e^{-z\bar{n}} H(z). \quad (2.21)$$

These generating functions are easily related to one another; for example, the following relation will prove to be useful:

$$H(z) = G(e^z) = \exp \{g(e^z)\}. \quad (2.22)$$

Finally, the so-called characteristic function $\Phi(t)$ is closely related to $H(z)$:

$$\Phi(t) = \sum e^{itn} P(n) = H(it). \tag{2.23}$$

It may be worth-while to remark that the factorial moments F_k vanish when k is larger than the maximum number of final particles \sqrt{s}/m ; this is not true for the other moments f_k , v_k and μ_k . Furthermore $G(z)$ is a polynomial in z even if s is large, but fixed.

Energy-momentum sum rules

Because of conservation laws, the inclusive distributions and correlations must obey sum rules. If P_μ is the energy momentum 4-vector of the initial state, energy momentum conservation easily leads to the following sum rules:

$$\int dp p_\mu N_1(p; s) = P_\mu. \tag{2.24}$$

The physical interpretation of this sum rule is clear: the energy-momentum of the produced particles must add up to the initial energy-momentum. The most general form of the sum rule reads:

$$\int dp p_\mu C_{k+1}(p, p_1, \dots, p_k; s) = (- \sum_{i=1}^k p_{i\mu}) C_k(p_1, \dots, p_k; s). \tag{2.25}$$

(For $k = 1$ one should take of course $C_1 = N_1$.) Integrating this equation k times we get:

$$\int \frac{p_{10}}{\sqrt{s}} dp_1 \dots dp_k C_k(p_1, \dots, p_k; s) = (-)^{k-1} (k-1)!. \tag{2.26}$$

This equation clearly shows that the k -particle correlation function cannot vanish identically.

Generalization to non-identical particles

Let me conclude this section by indicating briefly how the previous results are generalized in the case of non-identical particles. The general formulas will be obvious once you have seen them written in the case of 2 kinds of particles, say c and d . Let me first build the generating function:

$$G_{cd}(z_c, z_d) = \sum_{n_c, n_d} z_c^{n_c} z_d^{n_d} P(n_c, n_d). \tag{2.27}$$

The binomial moments F_{k_c, k_d} will be given by:

$$F_{k_c, k_d} = \frac{\partial^{k_c + k_d}}{\partial z_c^{k_c} \partial z_d^{k_d}} G_{cd}(z_c, z_d) \Big|_{z_c = z_d = 1} \tag{2.28}$$

and

$$F_{k_c, k_d} = \frac{1}{\sigma} \int \frac{d\sigma}{dp_1^c \dots dp_{k_c}^c dp_1^d \dots dp_{k_d}^d} dp_1^c \dots dp_{k_d}^d. \tag{2.29}$$

If one kind of particle (say d) is not detected in the experiment, one needs only set $z_d = 1$ in G_{cd} i.e.

$$G_{cd}(z_c, 1) = \sum_{n_c, n_d} z_c^{n_c} P(n_c, n_d) = \sum_{n_c} z_c^{n_c} P(n_c) = G_c(z_c). \quad (2.30)$$

On the contrary, if the experiment does not distinguish between c and d (for example if $c = \pi^+$, $d = \pi^-$ and one does not measure the sign of the charge), we have:

$$P(n) = \sum_{n=n_c+n_d} P(n_c, n_d),$$

$$G(z) = \sum_{n=n_c+n_d} z^n P(n_c, n_d) = G_{cd}(z, z). \quad (2.31)$$

Now, if $c = \pi^+$ and $d = \pi^-$, charge conservation imposes that $n_c = n_d$ so that $G_{cd}(z_c, z_d)$ is essentially a function of $z_c z_d$. More precisely (taking $c = +$, $d = -$) we have, if Q is the charge of the initial state ($Q \geq 0$):

$$G_{+-}(z_+, z_-) = \sum_{n_+ = n_- + Q} z_+^{n_+} z_-^{n_-} P(n_+, n_-),$$

$$G_{+-}(z_+, z_-) = (z_+)^Q G_-(z_+ z_-), \quad (2.32)$$

where G_- is generating function for negative particles. Thus, from (2.31), the generating function for all charged particles $G_c(z)$ is given by:

$$G_c(z) = G_{+-}(z, z) = z^Q G_-(z^2). \quad (2.33)$$

From (2.31) and (2.18) we get the relation between Mueller's moments of the charged MD and the negative MD:

$$\bar{n}_c = Q + 2\bar{n}_-,$$

$$f_2^c = -Q + 2f_1^- + 4f_2^-,$$

$$f_3^c = 2Q + 12f_2^- + 8f_3^-. \quad (2.34)$$

The most important point is that there are correlations coming from charge conservation alone: even if $f_2^- = 0$, we shall find $f_2^c \simeq \bar{n}_c$ at high energy. Hence it is probably better to study correlations between negative particles, in order to avoid this trivial effect.

Finally the energy-momentum sum rules will be modified in a rather obvious way; for example (2.24) becomes:

$$\int dp p_\mu (N_1^c(\mathbf{p}; s) + N_1^d(\mathbf{p}; s)) = P_\mu. \quad (2.35)$$

3. The short range order (SRO) hypothesis

As we shall see in the next Section, all the present experimental data can be understood in terms of a simple semi-empirical picture which, following Krzywicki [6], I shall call the short range order picture. In order to define precisely the SRO hypothesis, let me

consider the k -particle distribution $N_k(y_1, \dots, y_k, s)$, where I have integrated over the transverse momenta p_{Tk} and let me order the rapidities on the rapidity plot (Fig. 1):

$$y_b = y_0 \leq y_1 \leq y_2 \leq \dots \leq y_k \leq y_{k+1} = y_a.$$

N_k is *a priori* a function of $(k+1)$ rapidity differences which I can choose to be:

$$y_1 - y_0, y_2 - y_1, \dots, y_k - y_{k-1}, y_{k+1} - y_k. \tag{3.1}$$

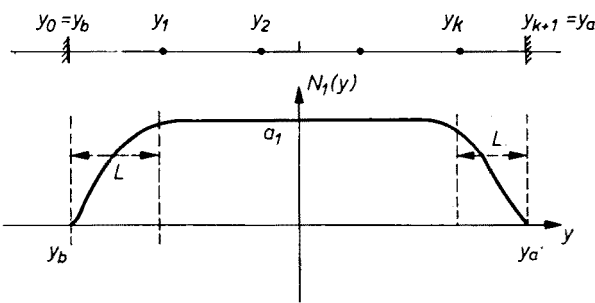


Fig. 1. Schematic plot of $N_1(y)$

Then the SRO hypothesis can be stated as follows:
 (SRO): If the rapidity difference $y_{i+1} - y_i, i = 1, \dots, k+1$, becomes large, then
 (1) N_k becomes independent of this variable and (2) it factorizes into a product of two terms:

$$N_k(y_1 - y_0, \dots, y_{k+1} - y_k) \simeq M_k^{(i)}(y_1 - y_0, \dots, y_i - y_{i-1}) \times \\ \times M_k^{(k-i)}(y_{i+2} - y_{i+1}, \dots, y_{k+1} - y_k), \tag{3.2}$$

where the superscript indicates the number of variables. Notice that the factorization hypothesis (2) implies of course the weaker statement (1), so that both statements should be tested experimentally.

Finally I must precise how large the rapidity difference is: (a) If $|y_1 - y_b|$ (or $|y_k - y_a|$) is larger than some characteristic length L , then N_k is independent of this variable. (b) If $|y_{i+1} - y_i|$ is larger than some characteristic length ξ , then N_k is independent of this variable.

One can get estimates for ξ from various considerations. In Mueller's theory, for example, one gets $\xi^{-1} \simeq \alpha_p(0) - \alpha_R(0) \simeq \frac{1}{2}$, where $\alpha_p(0)$ ($\alpha_R(0)$) is the intercept of the Pomeron (secondary Regge pole) trajectory. If the correlations are due to clustering, with isotropic decay of clusters, one gets $\xi \sim 1$ from the fact that the transverse momenta are limited to ~ 350 MeV/c. These estimates seem to be confirmed by experiment, and it is then useful to remember that, at least for pions

$$\xi \sim L \sim 1-2. \tag{3.3}$$

I shall first illustrate the SRO hypothesis on the simplest case, that of the one-particle inclusive distribution. N_1 is *a priori* a function of $y - y_b$ and $y - y_a$, but it should become independent of these variables when they are larger than L in absolute value. One can

then distinguish three different regions on the rapidity plot (assuming $Y \gg L$!, Fig. 1): (a) $|y - y_b| < L$; this region is known as the fragmentation region of b , where N_1 is a function of $y - y_b$ only. (b) $|y - y_a| < L$; fragmentation region of a , where N is a function of $y - y_a$ only. (c) $|y - y_a| > L$, $|y - y_b| > L$; central (or pionization) region, where N_1 should be independent of both $y - y_a$ and $y - y_b$; then N_1 is an energy independent constant. Of course this is nothing but the "old" scaling behaviour conjectured by

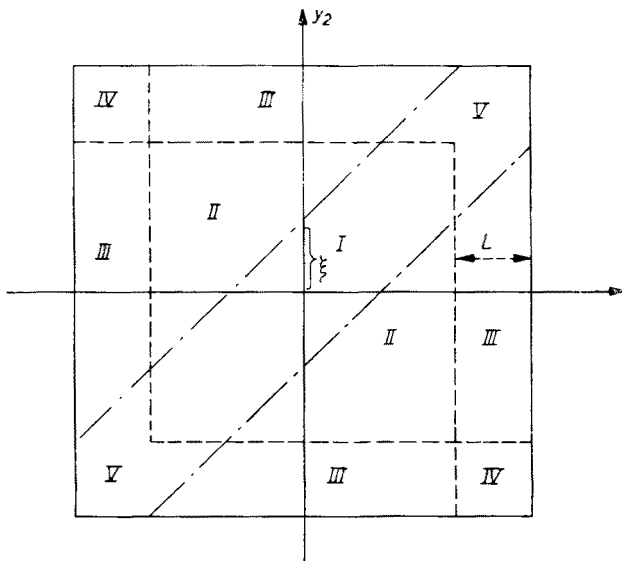


Fig. 2. Two-dimensional rapidity plot

Wilson [1], reformulated in terms of rapidity variables. Let me also remark that (a), (b) and (c) imply the logarithmic growth of the multiplicity:

$$\bar{n} = \int N_1(y) dy = a_1 Y + b_1. \quad (3.4)$$

The above discussion is probably familiar to everybody so that I can turn immediately to the more interesting case of 2-particle distributions. One can now separate the two-dimensional (y_1, y_2) rapidity plot into five regions (Fig. 2).

- I. y_1 and y_2 in the central region and $|y_1 - y_2| < \xi$: N_2 is a function of $(y_1 - y_2)$ only.
- II. y_1 and y_2 in the central region and $|y_1 - y_2| > \xi$: N_2 tends to a constant value: $N_2(y_1, y_2, s) = a'_2$.
- III. y_2 (for example) in the fragmentation region of a and y_1 in the central region: N_2 is a function of $(y_1 - y_2)$ only.

IV. y_1 in the fragmentation region of b (for example) and y_2 in the fragmentation region of a : N_2 is a function of $(y_1 - y_b)$ and $(y_2 - y_a)$, which factorizes into a product of two functions of $(y_1 - y_b)$ and $(y_2 - y_a)$ respectively: $N_2(y_1, y_2, s) = M_2^1(y_1 - y_b) M_2^1(y_2 - y_a)$. For two-particle correlations, this is the only result which depends on the factorization assumption.

V. y_1 and y_2 in the fragmentation region of a (for example): N_2 is a function of $(y_1 - y_a)$ and $(y_2 - y_a)$: $N_2(y_1, y_2, s) = M_2^2(y_1 - y_a, y_2 - y_a)$. This picture is of course oversimplified, and should hold only when the length of the rapidity plot is very large. However the important point is that ISR results are in qualitative agreement with this picture, as will be discussed in the next Section.

At this point, it is useful to make the connection between the SRO hypothesis, and a stronger assumption which has been often put forward in the past two years, and is known as the short range correlation (SRC) hypothesis. If one makes this assumption, one is then able to relate the two-particle inclusive distribution to one-particle distributions when the rapidity differences become large. Let me compare the predictions of SRO and SRC in the various regions of the rapidity plot.

I. Unchanged.

II. $N_2(y_1, y_2; s) = N_1(y_1)N_1(y_2) = a_1^2$. Notice that in region II the correlation $C_2(y_1, y_2)$ vanishes, and this is why I have called this assumption the SRC hypothesis.

III. $N_2(y_1, y_2; s) = N_1(y_2 - y_a) N_1(y_1) = a_1 N_1(y_2 - y_a)$.

IV. $N_2(y_1, y_2; s) = N_1(y_1 - y_b) N_1(y_2 - y_a)$.

V. Unchanged.

One can now draw important conclusions for the energy behaviour of Mueller's second moment f_2 , which is given by the integral of C_2 . One has only to remark that the area of region II increases as Y^2 , while the integral of C_2 over the other regions can grow at most as Y . Then from SRO (notice that one need not use the factorization assumption!):

$$\text{SRO: } f_2 = (a'_2 - a_1^2)Y^2 + O(Y). \quad (3.5)$$

If we now use the stronger SRC hypothesis, a'_2 is equal to a_1^2 ; the leading term in f_2 vanishes and we get

$$\text{SRC: } f_2 = \alpha_2 Y + O(1). \quad (3.6)$$

These results are easily generalized to the case of the k -particle distributions and to f_k . For example we would have from SRC, instead of (3.2)

$$\begin{aligned} N_k(y_1 - y_0, \dots, y_{k+1} - y_k) &= N_i(y_1 - y_0, \dots, y_i - y_{i-1}) \times \\ &\times N_{k-i}(y_{i+2} - y_{i+1}, \dots, y_k - y_{k+1}). \end{aligned} \quad (3.7)$$

Mueller's moments f_k behave as

$$\begin{aligned} \text{SRO: } f_k &= a_k Y^k + O(Y^{k-1}), \\ \text{SRC: } f_k &= \alpha_k Y + \beta_k. \end{aligned} \quad (3.8)$$

A theorem on the behaviour of partial cross-sections [7]

The energy behaviour of the partial cross-sections $\sigma_n(s)$ or more precisely of the ratio $\sigma_n(s)/\sigma(s)$, is strongly constrained if one adopts the SRC hypothesis.

Theorem: If one assumes that $f_k \sim \alpha_k Y$ for $k \leq 2N$ when Y is large, then the ratio σ_n/σ tends to zero at least as fast as Y^{-N} .

Proof: The idea of the proof is to show first that the central moment μ_{2N} increases at most as Y^N . In fact, we get from the very definition of μ_{2N} :

$$\mu_{2N} = \sum (n - \bar{n})^{2N} P(n) \geq (n_0 - \bar{n})^{2N} P(n_0),$$

where n_0 is some particular value of n ; since $(n_0 - \bar{n})^{2N}$ behaves as Y^{2N} , we immediately get that $P(n_0)$ must decrease at least as Y^{-N} . It remains to prove that μ_{2N} behaves as Y^N . Let me consider the generating function of the central moments $\tilde{H}(z, Y)$ (cf. (2.21) and (2.22))

$$\tilde{H}(z, Y) = e^{-z\bar{n}} H(z, Y) = \exp \left\{ -z\bar{n} + \sum_{k=1}^{\infty} \frac{(e^z - 1)^k}{k!} f_k \right\}.$$

Since $f_1 = \bar{n}$, $\tilde{H}(z, Y)$ has the following form:

$$\begin{aligned} \tilde{H}(z, Y) &= \exp \{ \lambda_2 z^2 + \lambda_3 z^3 + \dots \} = \\ &= (1 + \lambda_2 z^2 + \tfrac{1}{2} \lambda_2^2 z^4 + \dots)(1 + \lambda_3 z^3 + \dots), \end{aligned}$$

where $\lambda_i \sim Y$ if $i \leq 2N$. If one calculates μ_{2N} as

$$\mu_{2N} = \left. \frac{d^{2N}}{dz^{2N}} \tilde{H}(z, Y) \right|_{z=0},$$

the term with the highest power of Y will come from the derivation of $(N!)^{-1} \lambda_2^N z^{2N}$ so that μ_{2N} increases at most as Y^N .

In the SRC picture, all Mueller's moments f_k behave asymptotically as Y , so that the ratio σ_n/σ tends to zero faster than any inverse power of $Y = \ln s$ and we indeed expect the following behaviour [8]: $\sigma_n/\sigma \sim Y^n s^{-\alpha}$.

4. Experimental data and semi-empirical interpretation

The two-particle correlation $C_2(\mathbf{p}_1, \mathbf{p}_2; s)$ depends *a priori* upon 6 variables which I can choose to be $y_1, y_2, p_{1T}, p_{2T}, s$ and φ , where φ is the azimuthal angle:

$$\mathbf{p}_{1T} \cdot \mathbf{p}_{2T} = p_{1T} p_{2T} \cos \varphi. \quad (4.1)$$

Since a function of 6 variables is too complicated to be studied directly, one usually integrates over some variables. Thus I shall first examine rapidity correlations, integrating over transverse momenta; I shall then turn to azimuthal, or φ correlations. There may be other interesting kinds of correlations, but lack of time prevents me to study them in these lectures.

Rapidity correlations at "low" energy ($E_{\text{lab}} < 30$ GeV)

It is rather obvious that correlations would not be very interesting if they could be explained by already known effects. This is what happens if the incident energy is lower than 20–30 GeV in the lab system. There are two ways of showing that correlations at

such energies are already almost completely determined by the one-particle spectra and energy-momentum conservation: use the energy-momentum sum rules (2.25) which relate C_2 to N_1 or make calculations with a model which reproduces correctly the one-particle spectra, and does not contain correlations other than those due to energy-momentum conservation: this is the uncorrelated jet model (UJM).

The first method is model independent, but is less powerful. Because there is a factor p_0 in the integrand of (2.25) for $\mu = 0$, the constraints due to energy-momentum conservation are especially efficient in the fragmentation regions, where p_0 is large. At conventional accelerator energies, one sees only the fragmentation regions, so that we can expect strong constraints. Let me give the following example, taken from Caneschi [9]: from equation (2.26) we have

$$\int_0^1 C_k(x_1, \dots, x_k) \frac{dx_2}{x_2} \dots \frac{dx_k}{x_k} dx_1 \simeq 2(-)^{k-1}(k-1)!, \quad (4.2)$$

where

$$\bar{x} = \left(x^2 + \frac{4}{s} (m^2 + \bar{p}_T^2) \right)^{\frac{1}{2}}$$

while Mueller's moment f_k is given by

$$f_k \simeq \int_0^1 C_k(x_1, \dots, x_k) \frac{dx_1}{x_1} \dots \frac{dx_k}{x_k}. \quad (4.3)$$

If s is small enough, \bar{x} cannot approach zero (for example $0.2 \leq \bar{x} \leq 1$ if $s = 20 \text{ GeV}^2$) and the behaviour of f_k is almost completely determined by that of the integral in (4.2). We thus learn from kinematics alone that the moments f_k should alternate in sign at low energy, with $f_2 < 0$. This is in agreement with experiment.

The use of the UJM is of course more model dependent, since one has to choose a particular matrix elements, but leads to more quantitative results. Siverts and Thomas [10] have studied the correlations in 21 GeV/c proton-proton collisions, using the following matrix element for $pp \rightarrow pp + n\pi$:

$$|T|^2 = \left\{ \prod_{i=1}^2 e^{2\lambda p_{i0}/\sqrt{s}} f(p_{iT}) \right\} \left\{ \prod_{i=1}^n f(q_{iT}) \right\}, \quad (4.4)$$

where p_i and q_j represent the final proton and pion four-momenta. The first factor in (4.4) reproduces the leading particle effect, while the function $f(p_T)$ ensures the damping of transverse momenta; one particle spectra are then more or less correctly described by the matrix element (4.4).

The model reproduces at least in qualitative way the behaviour of the two-particle distribution $d\sigma/dy_1 dy_2$ (Fig. 3a) which shows that this distribution is essentially a kinematical reflection of already known effects. This is confirmed by the fact that the nova

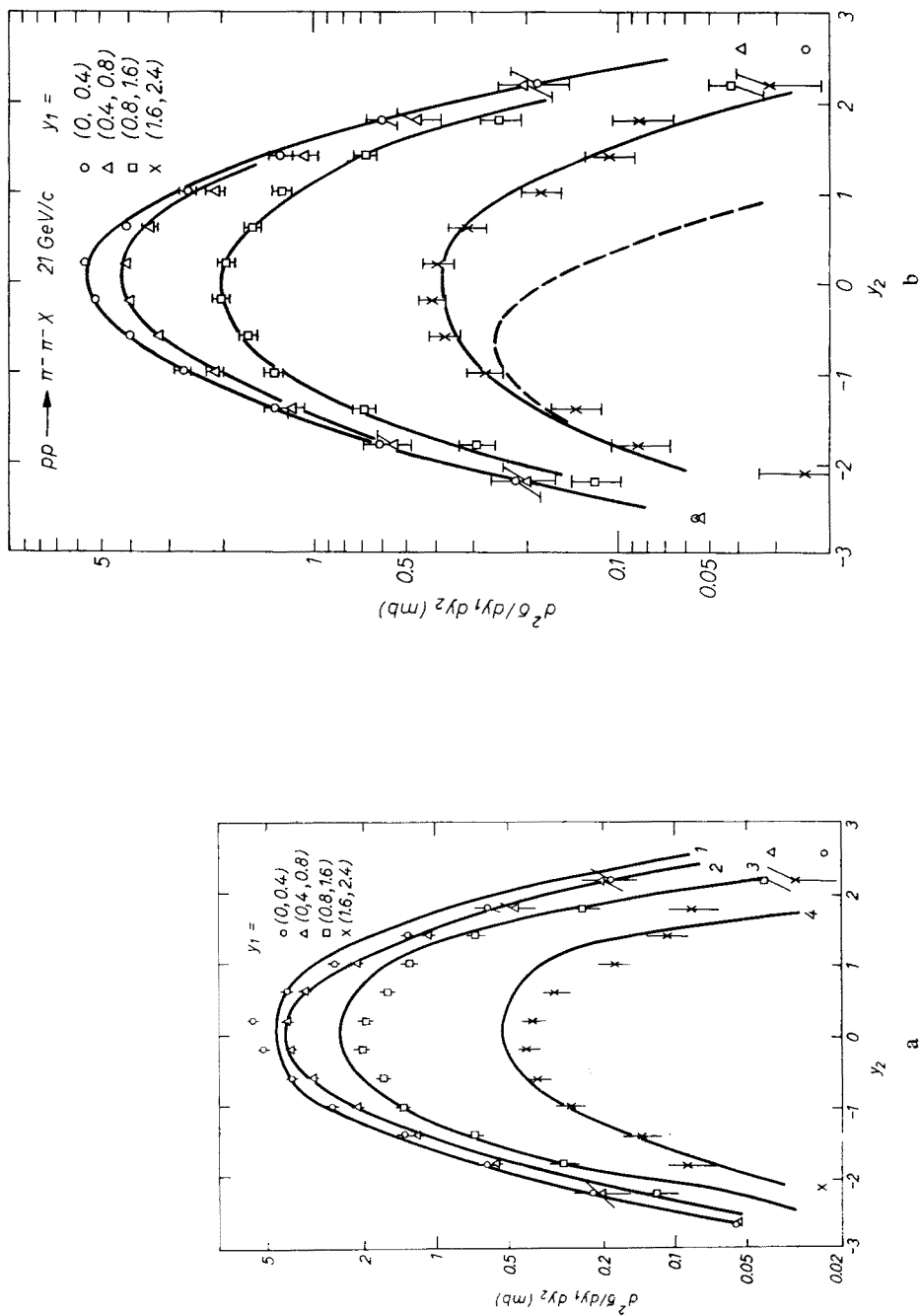


Fig. 3. a) Two-particle distribution in $pp-\pi^-\pi^-$ anything at 21 GeV/c, and fit by the uncorrelated jet model (Ref. [10]); b) Same distribution fitted by the nova model (Ref. [11])

model, which is based on completely different assumptions, but incorporates correctly the basic features of one-particle spectra and energy-momentum conservation, leads to a $d\sigma/dy_1dy_2$ in qualitative agreement with that found in UJM (Fig. 3b).

However, a more quantitative analysis reveals that the correlations predicted by UJM are too small in the region $y_1 \simeq y_2 \simeq 0$. This is an indication for dynamical effects, which show up very clearly in the ISR data.

Correlations between leading particles have been studied experimentally by the Aachen-Berlin-CERN-London-Vienna (ABCLV) collaboration [12] in the reaction

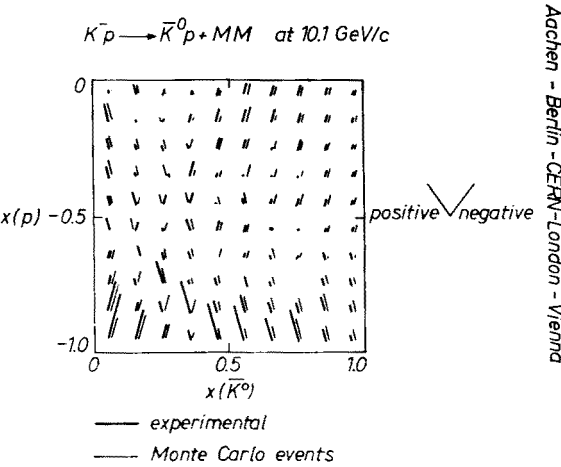


Fig. 4. Leading particle correlations in $K^-p \rightarrow \bar{K}^0 p + X$ (Ref. [11])

$K^-p \rightarrow \bar{K}^0 p + \text{anything}$ at 10 GeV/c. The results have been compared to a Monte-Carlo calculation using a matrix element similar to (4.4). Again the results of UJM are in qualitative agreement with experiment (Fig. 4).

This discussion makes it clear that one cannot learn much new physics by studying correlations at energy lower than 30 GeV. In such a range of energy, the exclusive analysis remains certainly the best tool in order to discover new properties of multiparticle production.

Rapidity correlation at ISR

Experiments have been recently performed at ISR, in order to measure two-particle correlations. The Pisa-Stony Brook (PSB) experiment measures correlation between all charged particles, while the CERN-Hamburg-Vienna (CHV) experiment [13] measures correlations between charged particles and protons. Finally the CERN-Holland-Lancaster-Manchester (CHLM) experiment measures correlations between leading protons with $0.6 \leq p_T \leq 1.1$ GeV and charged particles in the central region.

In the central region, the PSB and CHV experiments are in qualitative agreement, except for normalization problems in the PSB case. In fact the height of the one-particle rapidity plateau increases by 20–30% from $\sqrt{s} = 31$ GeV to $\sqrt{s} = 53$ GeV in this exper-

iment, while $d\sigma/dy_1 dy_2$ increases by $\sim 60\%$ in the same energy range. These results for one-particle distributions are in contradiction with single photon data, as well as with all single particle data obtained with spectrometers, which are consistent with an energy independent plateau.

Finally, in both experiments, one measures only the production angle of the charged particles, so that the true variable is not y , but rather $\eta = -\ln \tan \Theta/2$. In what follows I shall rely mainly on the results of the CHV experiment.

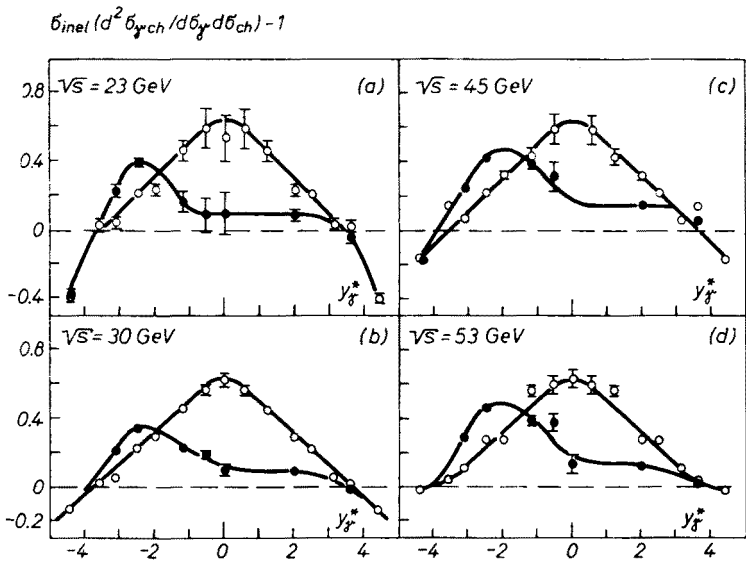


Fig. 5. Charged particle — photon correlations measured in the CERN–Hamburg–Vienna experiment (Ref. [13])

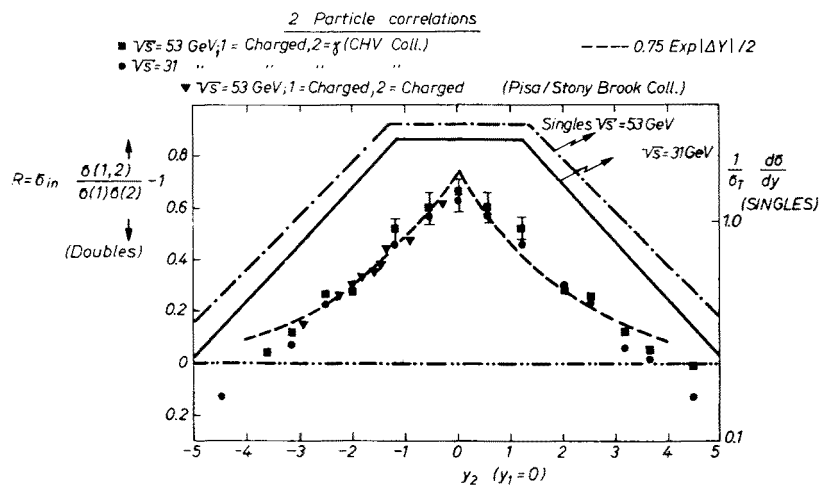


Fig. 6. Correlation length determination from CHV and PSB collaborations (Ref. [14])

On Fig. 5 one can see the ratio R defined as

$$R(y_1, y_2) = \frac{\sigma_{in} d\sigma/dy_1 dy_2}{d\sigma/dy_1 \cdot d\sigma/dy_2} - 1 = \frac{C_2(y_1, y_2)}{N_1(y_1)N_1(y_2)} \tag{4.5}$$

plotted as a function of $y_1 = y_Y^*$, for two values of $y_2 = y_{\text{charged}}$: $y_2 = 0$ and $y_2 = -2.5$, at various energies. (Incidentally, plotting the ratio R is not the best way of presenting data: it would be more useful to plot separately $d\sigma/dy_1 dy_2$, $d\sigma/dy_1$ and $d\sigma/dy_2$.) One can see at once that there is a rather strong positive correlation in the central region, where R may be as large as 0.6, and one can also see that this correlation is energy independent, since $d\sigma/dy_1$ and $d\sigma/dy_2$ are energy independent. The correlation decreases rapidly when $|y_1 - y_2|$ is large, and this decrease is compatible with the exponential law $C(|y_1 - y_2|) \sim$

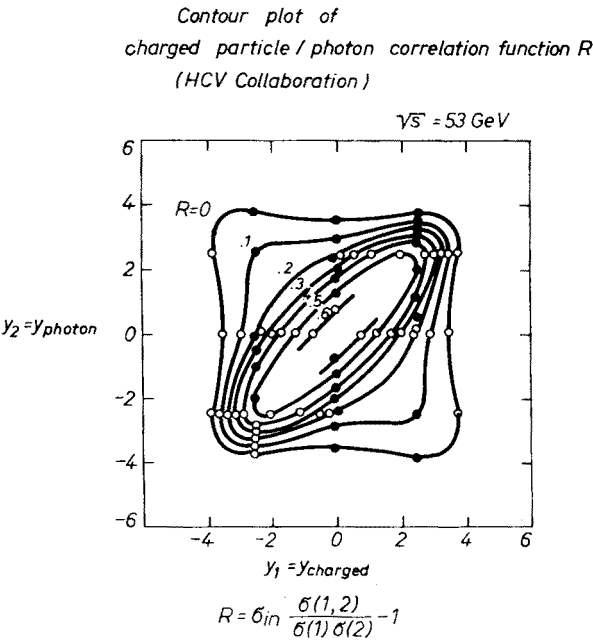


Fig. 7. Contour plot of the correlation in the CHV experiment (Ref. [14])

$\sim \exp(-|y_1 - y_2|/2)$ which means that the correlation length ξ is of order 2 (Fig. 6). The PSB results for R are in qualitative agreement with those of CHV, because the $\sim 60\%$ rise in $d\sigma/dy_1 dy_2$ is approximately cancelled by the $\sim 2 \times 25\%$ rise in $(d\sigma/dy_1)(d\sigma/dy_2)$.

A rather nice way of visualising the rapidity correlations is to make a contour plot in the (y_1, y_2) plane [14]. This contour plot is shown on Fig. 7 and one can see the following qualitative features.

When y_1 and y_2 belong to the plateau ($|y_i| \lesssim 1.5$), $N_2(y_1, y_2)$ is a function of $y_1 - y_2$ only, since the contours are roughly parallel to the line $y_1 = y_2$.

When $y_1 y_2 < 0$ and $|y_1 - y_2|$ larger than 2, the ratio R varies less rapidly with $|y_1 - y_2|$.

However the length of the rapidity plot is not large enough to see clearly the region II, where one expects $N_2(y_1, y_2)$ to tend to a constant value. Taking the maximum allowed value of y_1 and y_2 in the plateau ($y_1, -y_2 \simeq 1.5$) one can estimate that R would tend in region II to a constant equal to 0.2–0.3, which implies that

$$f_2^{+0} \simeq (0.2-0.3)\bar{n}_+^2. \quad (4.6)$$

When one of the rapidities (say y_2) moves into fragmentation regions, the contours are seen to become more parallel to the y_1 -axis. This means that R becomes a function of $y_2 - y_b$, but is independent of y_1 . This is most clearly seen on Fig. 5; taking $y_2 = -2.5$ (fragmentation region of b), one sees that R is independent of y_1 , within experimental errors.

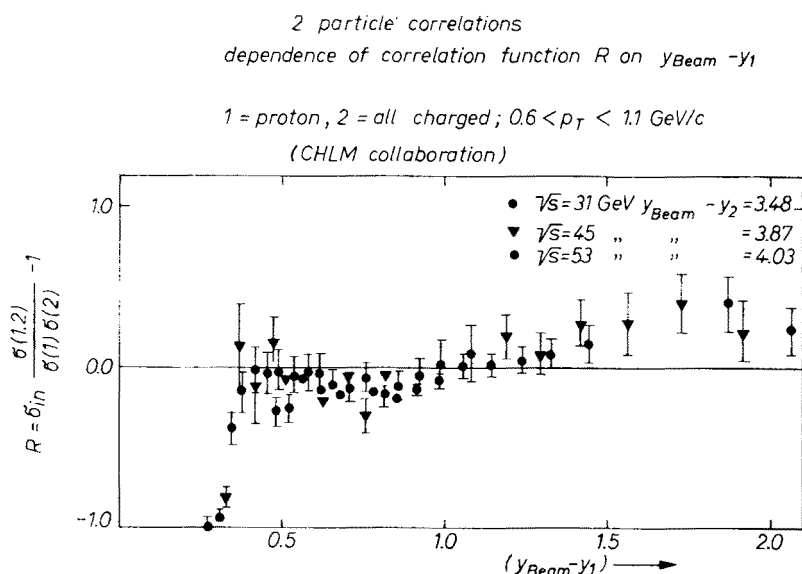


Fig. 8. Correlations between a leading proton and a charged particle at $y = 0$ measured in the CHLM experiment (Ref. [14])

in the interval $0 \lesssim y_1 \lesssim 2$. Since the one-particle distribution scales in the fragmentation region, one concludes that $N_2(y_1, y_2)$ is a function of $(y_2 - y_b)$ only when $|y_1 - y_2|$ is large and y_2 belongs to the central region.

The same effect appears also very clearly on Fig. 8, where one has plotted the ratio R for protons detected with $0.6 \leq p_T \leq 1.1$ in coincidence with a charged particle at $y_2 = 0$. In the laboratory frame, y_2 takes a different value at each energy, and Fig. 8 shows that the correlation depends only upon $|y_1 - y_a|$ and not on y_2 or s .

Finally there are also some partial tests of factorization; as they are not at present very accurate, I refer to the review paper of Sens [14] for a discussion.

To summarize, all the experimental data which are available at present indicate that the concept of short range order is approximately valid.

Azimuthal correlations

There are now some experimental data on azimuthal correlations, coming from the CHV experiment, which are worthwhile to examine in some detail. Let me first make some general remarks on azimuthal correlations [9].

Suppose that I take y_1 and y_2 in the central region, and that C_2 depends only upon $|y_1 - y_2|$. Then the energy-momentum sum rule (2.25), taken for $\mu = 1$ and $\mu = 2$, can be written as

$$-p_{1T}N_1(p_{1T}) = \int d|y_1 - y_2| dp_{2T} d\varphi p_{2T}^2 \cos \varphi C_2(|y_1 - y_2|, p_{1T}, p_{2T}, \varphi). \quad (4.7)$$

This equation tells us two important things:

if p_1 is fixed, C_2 must always have some dependence on φ , otherwise the RHS of (4.7) would vanish;

since $|y_1 - y_2|$ varies over a range $\sim \ln s = Y$, there is a potential logarithmic divergence in the RHS of (4.7). There are two completely different mechanisms to avoid this unwanted divergence.

(1) p_T is conserved locally: if particle 1 is produced with a large transverse momentum p_{1T} , transverse momentum conservation will be ensured by its nearest neighbours. Then the integral over $|y_1 - y_2|$ runs over a finite range and there is no divergence: in other words C_2 decreases rapidly when $|y_1 - y_2|$ is large. This is the mechanism chosen by the multiperipheral model: the momentum transfers t_i along the multiperipheral chain are minimal when the azimuthal angles between one particle and its neighbours are around π , and this configuration corresponds precisely to a large matrix element, because of the momentum transfer cut-off implied by the model.

(2) In the second mechanism, all produced particles cooperate to ensure transverse momentum conservation. This is the mechanism chosen by UJM; in this model the leading term (to the order $\ln s$) in C_2 is proportional to $p_{1T}p_{2T} \cos \varphi / \ln s$ and is independent of $|y_1 - y_2|$. Then the integral $\int d\varphi \cos \varphi C_2 \sim 1/\ln s$, and the divergence is again avoided.

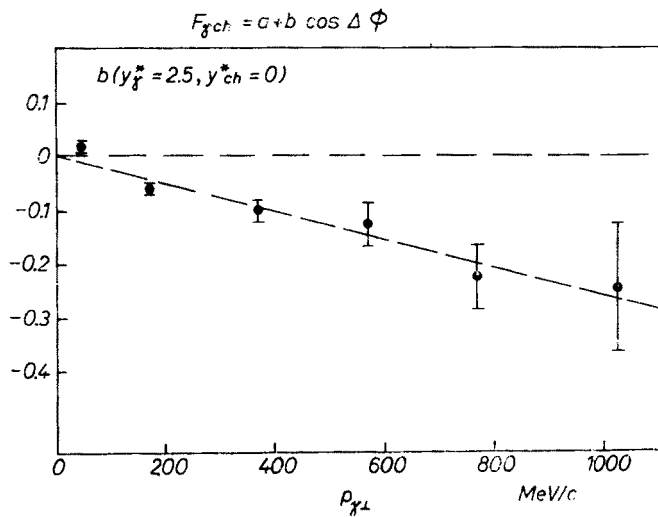
Now we can try to generalize the SRO picture if we assume that a mechanism of type (1) is realized in nature. We would then expect for example equations of the kind:

$$N_2(y_1, p_{1T}, y_2, p_{2T}, y_a, y_b) \simeq M_2^{(1)}(y_1 - y_b, p_{1T}) M_2^{(1)}(y_2 - y_a, p_{2T}), \quad (4.8)$$

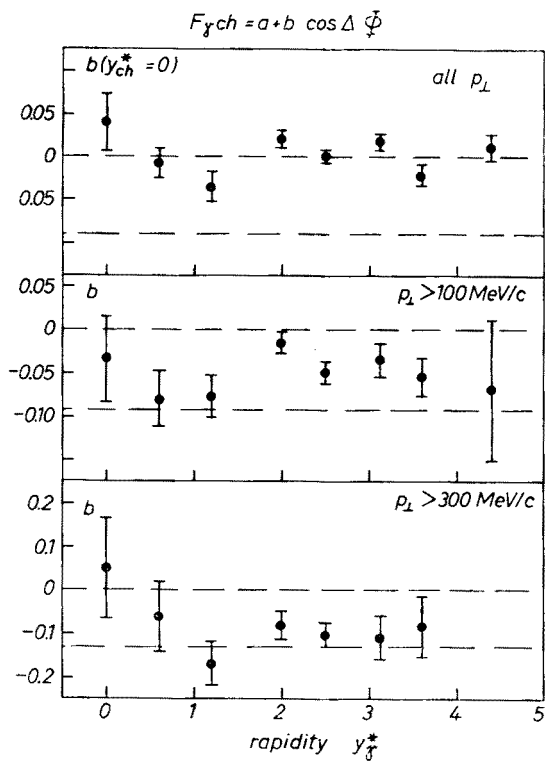
when $|y_1 - y_2|$ is large. In that case C_2 would be clearly independent of φ when $|y_1 - y_2|$ is large.

It is interesting to compare these expectations to the experimental data of the CHV collaboration. Let me define the two-particle distribution integrated over p_{2T} (since the experiment does not measure the transverse momentum of the charged particles) and integrate over p_{1T} from p_T^m to infinity:

$$N_2(y_1, y_2, p_T^m, \varphi) = \int_{p_T^m}^{\infty} p_{1T} dp_{1T} \int_0^{\infty} p_{2T} dp_{2T} N_2(y_1, y_2, p_{1T}, p_{2T}, \varphi). \quad (4.9)$$



a



b

Fig. 9. Azimuthal correlations: (a) unintegrated (b) integrated over p_{Ty} from p_T^m to ∞ (Ref. [13])

From (4.9) I define the ratio

$$R(y_1, y_2, p_T^m, \varphi) = \frac{N_2(y_1, y_2, p_T^m, \varphi)}{N_1(y_1, p_T^m)N_2(y_2)} - 1 \quad (4.10)$$

and approximate it by

$$R(y_1, y_2, p_T^m, \varphi) \simeq a' + b'(p_T^m, y_1, y_2) \cos \varphi. \quad (4.11)$$

The unintegrated ratio R will be

$$R(y_1, y_2, p_{1T}, \varphi) = \frac{N_2(y_1, y_2, p_{1T}, \varphi)}{N_1(y_1, p_{1T})N_2(y_2)} - 1 \simeq a + b(y_1, y_2, p_{1T}) \cos \varphi. \quad (4.12)$$

The coefficient $b(p_{1T})$ is plotted in Fig. 9a, while $b'(p_T^m)$ is given in Fig. 9b for $p_T^m = 0, 0.1$ and $0.3 \text{ GeV}/c$. It can be observed that this coefficient is different from zero (except when $p_T^m = 0$) even when $|y_1 - y_2|$ is large, and that there is no tendency for b to decrease when $|y_1 - y_2|$ increases. It seems that there is some long range effect which would contradict the SRO expectation (4.8). However, one must decide whether this effect is in some sense important, or small. One can for example use UJM, since this model is precisely at variance with (4.8), the coefficient b being even independent of $|y_1 - y_2|$. The UJM gives the following predictions for N_1 and N_2 in the central region [15]:

$$N_1(p_T) \simeq \frac{1}{2} f(p_T) e^{-p^2_T \Lambda^2 / 2Y} \simeq \frac{1}{2} f(p_T) \left(1 - \frac{p_T^2 \Lambda^2}{2Y} \right), \quad (4.13)$$

$$N_2(p_{1T}, p_{2T}) \simeq \frac{1}{4} f(p_{1T}) f(p_{2T}) \left(1 - \frac{\Lambda^2 (p_{1T}^2 + p_{2T}^2)}{2Y} - \frac{\Lambda^2 p_{1T} p_{2T} \cos \varphi}{Y} \right) \quad (4.14)$$

with:

$$\begin{aligned} \int p_T f(p_T) dp_T &= \frac{2}{\pi}, \\ \int p_T^3 f(p_T) dp_T &= \frac{2}{\pi \Lambda^2} = \frac{2}{\pi} \overline{p_T^2}. \end{aligned} \quad (4.15)$$

It is interesting to observe that the sum rule (4.7) is satisfied to leading order in $1/Y$ by (4.13) and (4.14). Then one easily obtains the following values of b :

$$b(p_{1T}) \simeq - \frac{\Lambda^2 \overline{p_T} p_{1T}}{Y}, \quad (4.16)$$

$$b'(p_T^m) \simeq - \frac{\Lambda^2 \overline{p_T}}{Y} \frac{\int_{p_T^m}^{\infty} p_T^2 f(p_T) dp_T}{\int_{p_T^m}^{\infty} p_T f(p_T) dp_T}. \quad (4.17)$$

As a particular case of (4.17) we have

$$b'(p_T^m = 0) \simeq -\frac{\Lambda^2 \bar{p}_T^2}{Y} = -\frac{\bar{p}_T^2}{p_T^2 Y}. \quad (4.18)$$

Taking $f(p_T) \sim e^{-6p_T}$ we can now compare the data to the predictions of the UJM. We find $b(p_{1T}) \sim 0.25 p_{1T}$, $b'(p_T^m = 0) \sim 0.08$, $b'(p_T^m = 0.1) \sim -0.09$, $b(p_T^m = 0.3) \sim -0.13$. Except for the case $p_T^m = 0$, the estimates of UJM are not so far from the data, which might suggest that SRO cannot be generalized when one wishes to take into account transverse momenta.

5. Multiplicity distributions

As we have seen in Section 2, the study of multiplicity distributions (MD) is complementary to that of correlations, since it gives information on their integrals. I wish to show now, how the experimental data for MD also confirm the SRO hypothesis.

Experimental data for MD are available at 50, 69, 102, 205 and 303 GeV/c in pp collisions [16], and also at 40, 50 and 200 GeV/c in πp collisions [17]. I shall use mainly the pp results, which are more detailed and which I happen to know best.

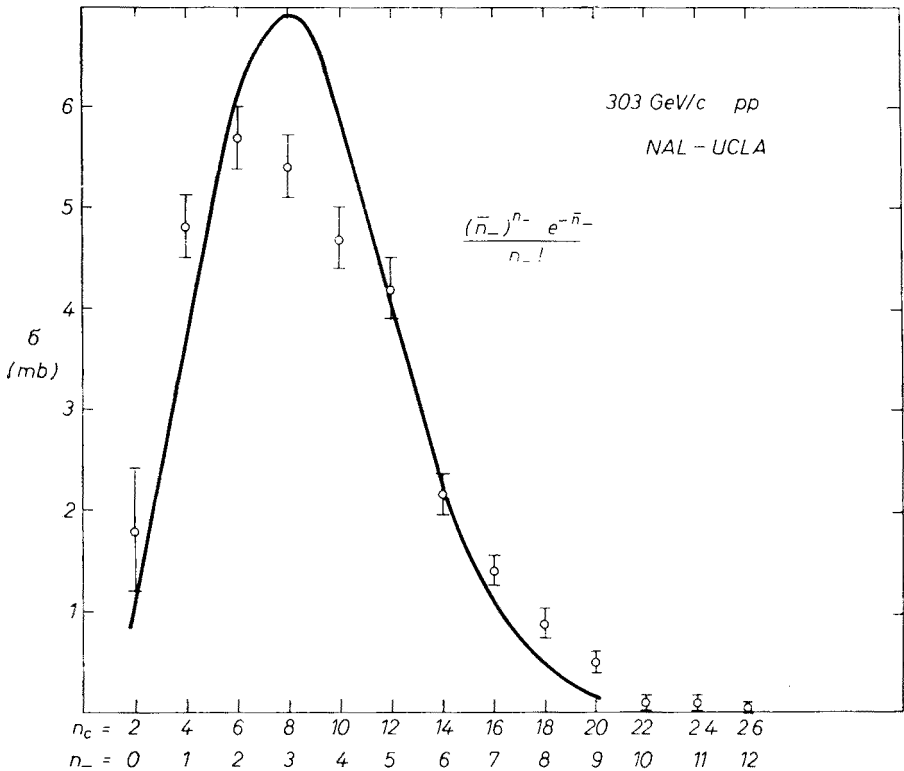


Fig. 10. Multiplicity distribution at 303 GeV/c and fit by a Poisson distribution in n_- (Ref. [16])

The MD can be displayed either as a function of the number of charged particles n_c , or of negative particles n_- , which are related by $n_c = 2n_- + 2$ in pp collisions. A typical MD at 303 GeV/c is shown on Fig. 10, where it is compared to a Poisson distribution with the same mean value \bar{n}_- .

Empirical regularities

Although the variable n_- is preferred by most theorists, it seems that empirical regularities appear in the MD when one uses the variable n_c ; in fact it seems that some definite asymptotic features appear in the MD when the energy is larger than 30–40 GeV in the

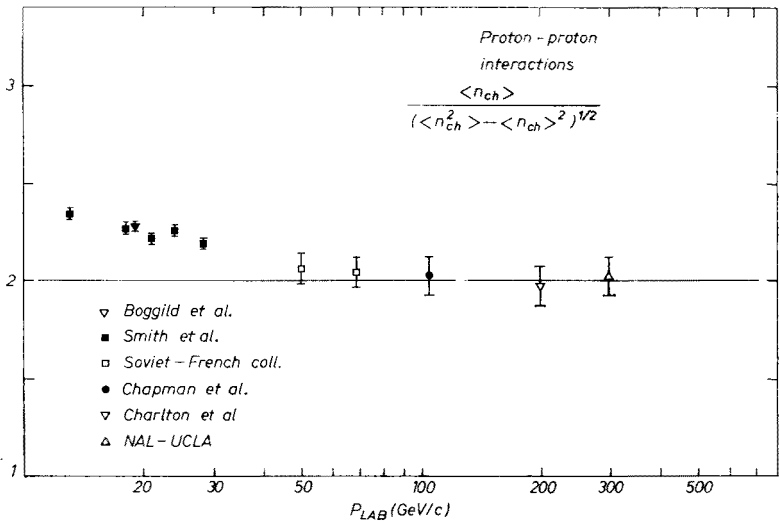


Fig. 11. Ratio D_c/\bar{n}_c (Ref. [16])

lab system, and when one uses the variable n_c ; a good explanation of these observations is still lacking.

Czyżewski and Rybicki and Wróblewski [18] have noticed that the ratio \bar{n}_c/D_c , where D_c is the dispersion

$$D_c = (\mu_2^c)^{\frac{1}{2}} = (\overline{n_c^2} - \bar{n}_c^2)^{\frac{1}{2}}$$

is constant and equal 2 within experimental errors above 50 GeV/c. This ratio is also somewhat larger than 2 at conventional accelerator energies, which seems to imply that some asymptotic feature of the MD is indeed reached above 30–40 GeV/c (see Fig. 11).

The equation $D_c/\bar{n}_c = 0.5$ can also be written as $\bar{n}_c^2 = 1.25 \bar{n}_c^2$ and it is remarkable that this relation generalizes to higher moments:

$$\overline{n_c^k} = c_k \bar{n}_c^k, \tag{5.1}$$

where c_k is energy independent from 50 to 300 GeV/c. The following values of c_k have been calculated by Slattery [19], using the 50–300 GeV/c data.

$$\begin{array}{lll}
c_2 = 1.244 \pm 0.006 & c_3 = 1.813 \pm 0.020 & c_4 = 2.97 \pm 0.06 \\
c_5 = 5.36 \pm 0.15 & c_6 = 10.4 \pm 0.4 & c_7 = 21.6 \pm 1.1 \\
c_8 = 47.0 \pm 2.8 & c_9 = 107 \pm 7.8 & c_{10} = 252 \pm 22
\end{array}$$

However, higher moments are very sensitive to the tail of MD, and (5.1) should not be taken too seriously for $k \gtrsim 4$.

Another interesting feature is the behaviour of f_2^- . If Q is the charge of the initial state, we have seen that

$$\begin{aligned}
\bar{n}_c &= 2\bar{n}_- + Q, \\
D_c^2 &= f_2^c + \bar{n}_c = 4f_2^- + 2\bar{n}_c - 2Q.
\end{aligned} \tag{5.2}$$

Using the empirical relation $D_c = 0.25 \bar{n}_c^2$ we get

$$f_2^- = 0.25 \bar{n}_-^2 - 0.5 \bar{n}_- + 0.25. \tag{5.3}$$

Thus f_2^- is positive and increases as $\bar{n}_-^2 \sim Y^2$ when the energy of the collision is large. Experimentally f_2^- is positive for $E_L \geq 50$ GeV ($\bar{n}_- \geq 1.66$), which means that the MD is then broader than Poisson. The fact that f_2^- is negative at low energy is to be expected from 4-momentum conservation, as was explained at the beginning of the last Section.

KNO scaling

Koba, Nielsen and Olesen (KNO) have made the observation that the behaviour (5.1) can be derived asymptotically from SRO, and were able to propose a kind of scaling law for the MD, which is remarkably satisfied by the data.

In fact, from the SRO hypothesis (and even from the first part of it) we get that

$$F_k = \frac{1}{\sigma} \int \frac{d\sigma}{dy_1 \dots dy_k} dy_1 \dots dy_k \sim Y^k \tag{5.4}$$

or $F_k \sim c_k \bar{n}^k$. The proof of (5.4) was discussed in Section 3 for $k = 2$, and is obviously generalized to any value of k . Of course (5.4) is a very asymptotic result! Equation (5.4) has a simple and exact solution in the form of a compound Poisson distribution [21]: the MD $P(n, \bar{n})$ is given by

$$P(n, \bar{n}) = \int \frac{dx}{\bar{n}} f\left(\frac{x}{\bar{n}}\right) \frac{e^{-x} x^n}{n!}, \tag{5.5}$$

where $f(x)$ is defined by its moments

$$c_k = \int_0^\infty x^k f(x) dx. \tag{5.6}$$

However, this is not the solution chosen by KNO, since experimentally one does not have $F_k = c_k \bar{n}^k$ but rather (5.1). Of course both equations are asymptotically identical, but it might be preferable to start from that which is satisfied by the data. Let us then assume

that $\bar{n}^k = c_k \bar{n}^k$ and define a probability density $p(x, \bar{n})$ by [22]

$$p(x, \bar{n}) = \sum_n P(n, \bar{n}) \delta\left(x - \frac{n}{\bar{n}}\right) \tag{5.7}$$

whose moments v_k are simply c_k . The characteristic function $\varphi(t, \bar{n})$ of $p(x, \bar{n})$ is directly given by the c_k 's:

$$\varphi(t, \bar{n}) = \int_{-\infty}^{\infty} e^{itx} p(x, \bar{n}) dx = \sum c_k \frac{(it)^k}{k!}. \tag{5.8}$$

Equation (5.8) shows that $\varphi(t, \bar{n})$ is indeed independent of \bar{n} , so that its inverse Fourier transform $p(x, \bar{n})$ is also independent of \bar{n} :

$$p(x, \bar{n}) = \frac{1}{2\pi} \int_{-\infty}^{\infty} e^{-itx} q(t) dt = \psi(x), \tag{5.9}$$

where $\psi(x)$ is defined by (5.9). We thus have KNO scaling:

$$P(n, \bar{n}) = \frac{1}{\bar{n}} \psi\left(\frac{n}{\bar{n}}\right), \tag{5.10}$$

where $\psi(x)$ is completely defined by the c_k 's, and must satisfy the relations

$$\int_0^{\infty} \psi(x) dx = \int_0^{\infty} x \psi(x) dx = 1. \tag{5.11}$$

Equation (5.10) is valid to the order $1/\bar{n}^2$, for two reasons: first we should have $\bar{n}^k = c_k \bar{n}^k + O(\bar{n}^{k-1})$ and secondly we have identified the continuous variable x in (5.9) with the discrete variable $1/\bar{n}$. In fact $P(n, \bar{n})$ given by (5.10) is not in general a probability distribution since $\sum P(n, \bar{n}) \neq 1$, even if (5.11) is satisfied. However, the error will be of order $1/\bar{n}^2$ if $\psi(0) = 0$, since the Riemann sum and the integral of $\psi(x)$ differ by $1/\bar{n}^2$, not $1/\bar{n}$, in that case.

Let me illustrate the formalism on a simple case: assume that $c_k = k!$; then

$$\varphi(t) = \sum_k k! \frac{(it)^k}{k!} = \frac{1}{1-it}$$

and

$$\psi(x) = e^{-x} \theta(x), \quad P(n, \bar{n}) = \frac{1}{\bar{n}} e^{-n/\bar{n}}.$$

Although one would expect $1/\bar{n}$ corrections to the scaling law (5.10), experimental data are in excellent agreement with (5.10) from 50 to 300 GeV, showing the approximate

validity of early KNO scaling. A very good fit ($\chi^2 \lesssim 1$ per point) is obtained with the following limiting function [23] (provided the variable $n = n_c$):

$$\psi(x) = Ax^\beta e^{-yx^2}. \quad (5.12)$$

This is a one parameter fit since $\psi(x)$ must satisfy the normalization conditions (5.11); Weisberg finds that $\beta \simeq 1.1$ – 1.2 gives an excellent fit to the data.

Density correlations

An interesting observation has been made recently by Weingarten [24] in connection with the KNO scaling. Starting from the ordinary moments v_k , one can define moments K_k exactly as one defines f_k from F_k :

$$H(z, \bar{n}) = \sum_k v_k \frac{z^k}{k!} = \exp \left\{ \sum_k K_k \frac{z^k}{k!} \right\}. \quad (5.13)$$

These moments are nothing but the cumulants of the MD. Then from (5.1):

$$H(z, \bar{n}) = \sum_k c_k \frac{(z\bar{n})^k}{k!} = \exp \left\{ \sum_k y_k \frac{(z\bar{n})^k}{k!} \right\}. \quad (5.14)$$

The values of y_2 , y_3 and y_4 have been calculated by Slattery [19] who finds:

$$\frac{1}{2!} y_2 = 0.122 \pm 0.003, \quad \frac{1}{3!} y_3 = (1.34 \pm 0.07) \cdot 10^{-2}, \quad \frac{1}{4!} y_4 = (3.9 \pm 1.4) \cdot 10^{-4}.$$

It thus appears that the coefficients $y_k/k!$ decrease quickly with k and that $y_4/4!$ is already negligible. Weingarten has shown that the coefficients c_4 to c_{10} can be calculated to a good approximation from y_2 and y_3 alone. Then it is sufficient to keep the first three terms (with $y_1 = 1$ by definition) in (5.14) in order to obtain the generating function H to an excellent approximation. Similarly one can write the characteristic function $\varphi(t)$ in (5.8) as follows:

$$\varphi(t) = \exp \left(it - \frac{1}{2!} y_2 t^2 - \frac{i}{3!} y_3 t^3 \right). \quad (5.15)$$

From this form for $\varphi(t)$ one can calculate $\psi(x)$ by making a Fourier transform; the result shown in Fig. 12a gives a very good fit to the experimental MD. Keeping only y_2 would lead to a Gaussian form for $\psi(x)$, but the agreement with the data is then much poorer.

Weingarten's work shows why it is possible to obtain a scaling function $\psi(x)$ depending only upon a few parameters. Furthermore Koba and Weingarten [25] have shown that the y 's can be obtained as integrals of quantities called "density correlations", which are not submitted to kinematical constraints as the usual correlations. Then one may set $y_k = 0$ without any problem.

However this work does not shed any light on the reason why early KNO scaling is experimentally valid, and why the variable n_c plays such a privileged role (early KNO

scaling is not very good with the variable n_-). It could well be that the validity of KNO scaling is a mere accident, and in what follows I shall give two other possibilities, which also give good fits of the MD, but do not satisfy early KNO scaling. Nevertheless the KNO parametrization (5.10) remains at present the simplest parametrization of experimental data.

Short range correlations and clustering

The first alternative to KNO is based on the short range correlation hypothesis. After my previous emphasis on SRO, it may seem surprizing that I come back to SRC: actually the present experimental data do not disprove SRC, although I do not think that this

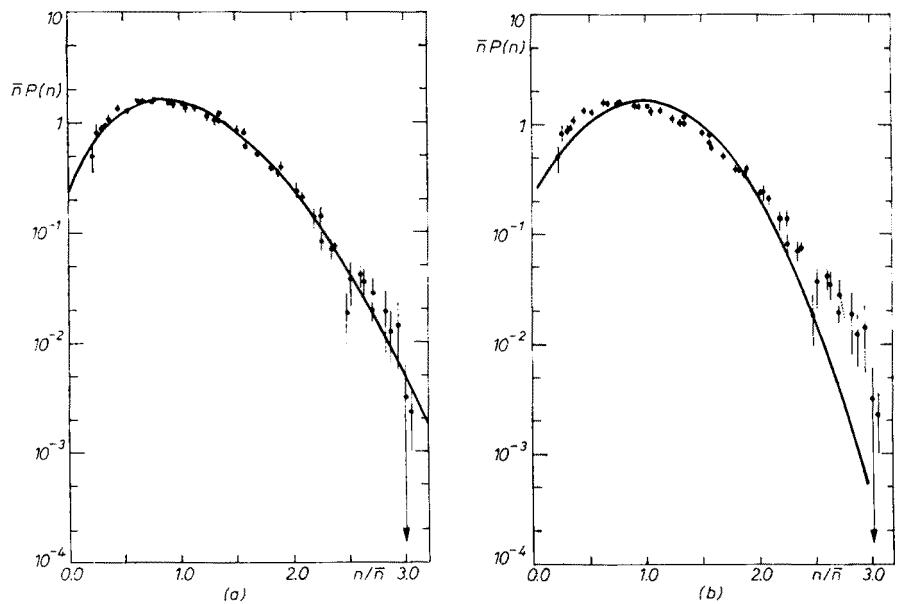


Fig. 12. KNO scaling from Weingarten's fit (Ref. [24])

assumption will continue to stand against forthcoming experiments. It has been shown by Slattery [19] and Weisberger [26] that Mueller's moments can be fitted by the linear formula

$$f_k = \alpha_k \bar{n} + \beta_k \tag{5.16}$$

predicted by SRC (Fig. 13). There is a possible physical interpretation of the coefficients α_k which I would like to discuss now. The idea is to assume that particle production occurs *via* clusters which decay into the observed particles. Let $\tilde{P}(m)$ be the probability of producing m clusters and $\tilde{G}(z)$ the corresponding generating function. I call w_j the probability that a given cluster decays into exactly j (identical) particles, and I construct the generating function $\lambda(z)$:

$$\lambda(z) = \sum_{j=0}^{\infty} z^j w_j, \quad \lambda(1) = 1. \tag{5.17}$$

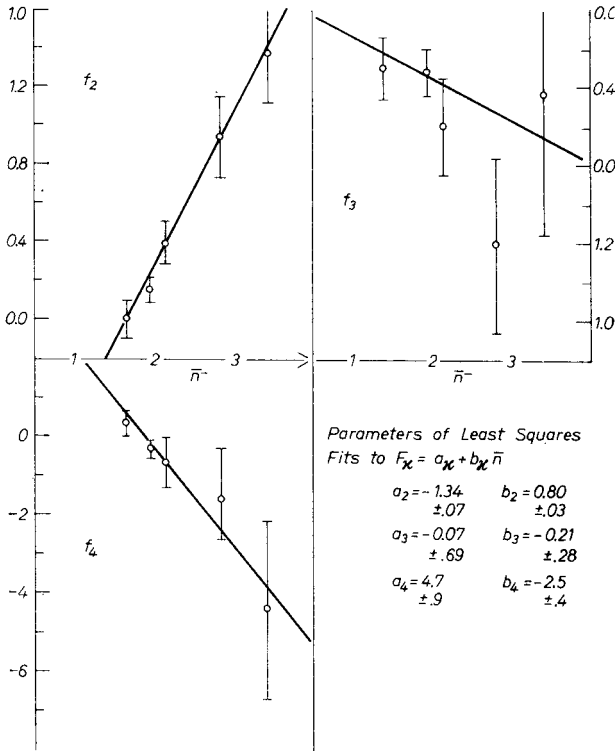


Fig. 13. Linear fit of Mueller's moments f_k^- (Ref. [26])

The probability $P(n, m)$ that m clusters decay into n final particles is $P(n, m) = \sum_{j_1 \dots j_m} w_{j_1} \dots w_{j_m} \delta(n - j_1 - \dots - j_m)$ so that

$$\sum_n z^n P(n, m) = (\lambda(z))^m. \quad (5.18)$$

I can now compute the generating function $G(z)$:

$$G(z) = \sum_n z^n P(n) = \sum_{n,m} z^n P(n, m) P(m) = \sum_m (\lambda(z))^m \tilde{P}(m)$$

and we get the important relation:

$$G(z) = \tilde{G}(\lambda(z)). \quad (5.19)$$

Assume for example that the clusters are produced independently, so that $\tilde{G}(z) = \exp(\bar{m}(z-1))$. Then

$$G(z) = \exp[\bar{m}(\lambda(z)-1)] \quad (5.20)$$

and making a Taylor expansion around $z = 1$ we find

$$\overline{m}(\lambda(z)-1) = \sum_{k=1}^{\infty} \frac{(z-1)^k}{k!} \overline{m}\lambda^{(k)}(s)$$

so that

$$f_k = \overline{m} \left. \frac{d^k \lambda}{dz^k} \right|_{z=1} = \overline{m} \overline{j(j-1) \dots (j-k+1)}. \quad (5.21)$$

For example, if $w_j = \delta_{j,j_0}$ i. e. if a cluster decays always into exactly j_0 particles we have

$$f_k = \overline{m} j_0(j_0-1) \dots (j_0-k+1) \quad (5.22)$$

and we find $f_k = 0$ for $k \geq j_0+1$. From the Weisberger fit to f_2^- we find $f_2^- \simeq 0.8 \bar{n}_- \simeq \simeq (j_0-1) \bar{n}_-$. Then if our picture is the correct one, there are on the average 1.8 negative pions in a cluster; this would suggest a model where the clusters contain 5–6 pions. It is easy to generalize (5.19) to the case of non-identical particles. If $\lambda(z_c, z_d)$ is the generating function for the cluster decay into two kinds of particles, c and d , we have

$$G(z_c, z_d) = \tilde{G}(\lambda(z_c, z_d)) \quad (5.23)$$

and

$$f_{k_c, k_d}^{c, d} = \overline{m} \overline{j_c(j_c-1) \dots (j_c-k_c+1) j_d \dots (j_d-k_d+1)}. \quad (5.24)$$

The diffraction + pionization model

While the SRC model discussed above is possibly valid with σ_{in} as the normalization cross-section, it is certainly ruled out by the data if one chooses σ_T instead of σ_{in} ; because of the theorem proved at the end of Section 3, the elastic cross-section should be rapidly decreasing with energy, which is certainly not the case. Let me recall that the theoretical models which predict SRC would like to use σ_T as a normalization cross-section, and not σ_{in} . Having already subtracted σ_{el} to pass from σ_T to σ_{in} , one is naturally led to subtract also the cross-section for diffractive processes and to build the so-called diffraction + pionization model (DPM) [27].

In this model, one assumes that any event is either of the diffractive (D) or of the pionization (π) kind, and that the two mechanisms should be added independently (for another version of DPM, see the paper by A. Morel in this issue). The partial cross-section σ_n is then written as $\sigma_n = \sigma_n^D + \sigma_n^\pi$. One generally assumes that the multiplicity of diffractive events is finite, while the pionization component obeys the SRC hypothesis; the corresponding multiplicity \bar{n}_π is then logarithmic. For the sake of simplicity, some authors assume a Poisson distribution for σ_n^π , but this is certainly not required by the model.

It is easy to calculate the behaviour of Mueller's moments:

$$f_1 = \bar{n} = \frac{1}{\sigma} \sum (n \sigma_n^D + n \sigma_n^\pi) = \frac{\sigma_D}{\sigma} \sum n \frac{\sigma_n^D}{\sigma_D} + \frac{\sigma_\pi}{\sigma} \sum n \frac{\sigma_n^\pi}{\sigma_\pi}$$

or

$$\bar{n} = \alpha \bar{n}_D + (1 - \alpha) \bar{n}_\pi, \quad (5.25)$$

where $\alpha = \sigma_D/\sigma$ is the relative amount of diffraction. The calculation of f_2 is quite similar:

$$f_2 = \alpha \overline{n(n-1)}_D + (1 - \alpha) \overline{n(n-1)}_\pi - (\alpha \bar{n}_D + (1 - \alpha) \bar{n}_\pi)^2.$$

The most interesting point is the high energy behaviour of f_2 : since in the pionization component $\overline{n(n-1)}_\pi = \bar{n}_\pi^2 + O(\bar{n}_\pi)$, we have

$$f_2 \simeq (1 - \alpha) \bar{n}_\pi^2 - (1 - \alpha)^2 \bar{n}_\pi^2 = \alpha(1 - \alpha) \bar{n}_\pi^2 = \frac{\alpha}{1 - \alpha} \bar{n}^2. \quad (5.26)$$

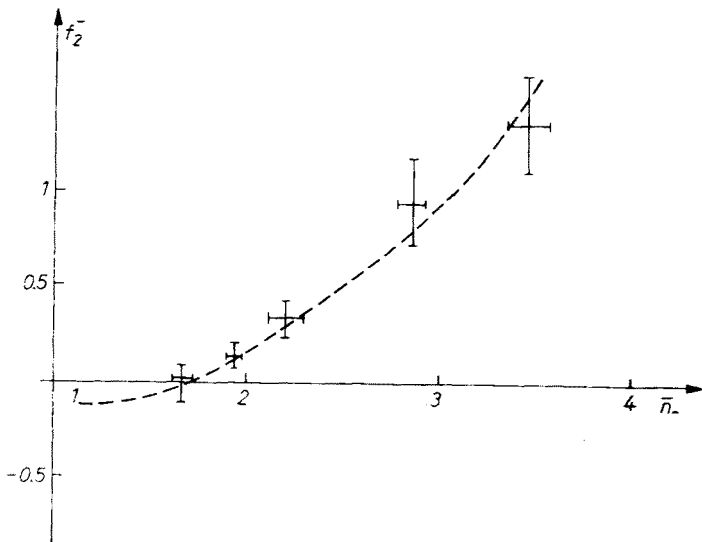


Fig. 14. f_2^- in the diffraction + pionization model (Ref. [28])

We thus get the important result that f_2 behaves as \bar{n}^2 in DPM. More generally f_k behaves as \bar{n}_k ; for example:

$$f_3 = \frac{\alpha(2\alpha - 1)}{(1 - \alpha)^2} \bar{n}^3 + O(\bar{n}^2),$$

$$f_4 = \frac{\alpha(1 - 6\alpha + 6\alpha^2)}{(1 - \alpha)^3} \bar{n}^4 + O(\bar{n}^3). \quad (5.27)$$

Let me give some details of the fits for the MD obtained by various groups.

Fiałkowski *et al.* [28] assume a Poisson distribution for σ_n^π . Then the only parameters are the diffractive cross-sections σ_n^D ; the only important diffractive cross-sections are σ_0^D , σ_1^D , σ_2^D : $\sigma_0^D = 2.3 \pm 0.5$, $\sigma_1^D = 3.1 \pm 0.4$, $\sigma_2^D = 1.7 \pm 0.7$, ($\sigma_3^D = 0.6 \pm 0.3$) (mb). The total diffractive cross-section is then estimated to be of the order of 7 mb. This means that

$\alpha = \sigma_D/\sigma_{in} \simeq 0.22$: diffraction represents 22% and pionization 78% of the total inelastic cross-section. The parameter f_2^π is in very good agreement with experiment (Fig. 14).

The results of Frazer *et al.* [29], who also use a Poisson distribution for σ_n^π , are very similar to those of Fiałkowski. They find $\alpha = 0.19$ and $\sigma_0^D = 2.0$, $\sigma_1^D = 2.7$, $\sigma_2^D = 1.7$ (mb).

The most important prediction is that of a dip which appears in the MD at the highest ISR energy (Fig. 15): at high energy the diffractive component becomes clearly separated from the pionization one, leaving a dip between both distributions [27]. However this

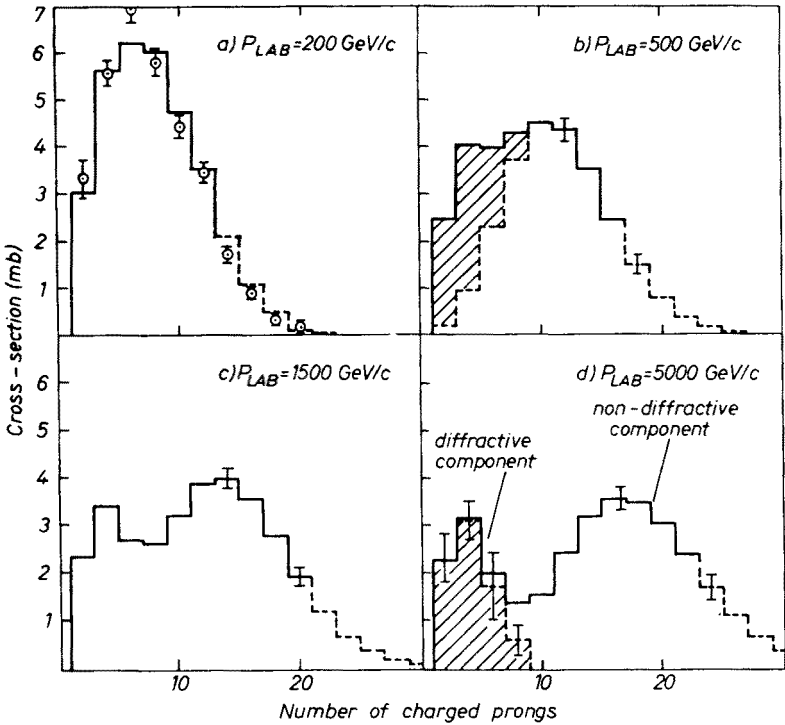


Fig. 15. Multiplicity distribution in the diffraction + pionization model (Ref. [28])

prediction depends in a crucial way on the assumption that σ_n^D is energy independent; in view of recent ISR data on the inelastic proton spectrum, this may be an oversimplification.

Harari and Rabinovici [30] assume that f_2^π is non zero and parametrize f_2^π as follows: $f_2^\pi = c_2 \bar{n}_\pi + d_2$. In other words they take non-zero correlations for the pionization component. The main parameters are again σ_0^D , σ_1^D , σ_2^D and also c_2 and d_2 . Since part of the correlations comes from the pionization component, the value found for α is slightly lower: $\alpha = 0.16$ while the results for σ_n^D are: $\sigma_0^D = 2.0$, $\sigma_1^D = 2.2$, $\sigma_2^D = 0.9$ (mb). In any case the introduction of the non zero f_2^π does not change the qualitative features of the fit, and a dip in the MD is again predicted at the highest ISR energies.

In conclusions the DPM model gives a satisfactory fit of the MD with a small number of parameters. This fit does not satisfy early KNO scaling since the limiting function

$\psi(x)$ is

$$\psi(x) = \alpha\delta(x) + (1-\alpha)\delta\left(x - \frac{1}{1-\alpha}\right)$$

and this limit is clearly very far from being reached, even at ISR.

Some difficulties with DPM may arise when one considers higher moments of the MD. For example f_3^- tends to be more negative in DPM than in experiments, since

$$f_3^- \simeq \frac{\alpha(2\alpha-1)}{(1-\alpha)^2} \bar{n}_-^3 \simeq -0.20\bar{n}_-^3.$$

However, these difficulties may be ascribed to phase space effects.

Further discussion of the model: correlations

It is easy to obtain the form of correlations in DPM. One begins by defining the diffractive and pionization one and two-particle distributions:

$$\begin{aligned} N_1^D(y) &= \frac{1}{\sigma_D} \frac{d\sigma^D}{dy}, & N_1^\pi(y) &= \frac{1}{\sigma_\pi} \frac{d\sigma^\pi}{dy}, \\ N_2^D(y_1, y_2) &= \frac{1}{\sigma_D} \frac{d\sigma^D}{dy_1 dy_2}, & N_2^\pi(y) &= \frac{1}{\sigma_\pi} \frac{d\sigma^\pi}{dy_1 dy_2}. \end{aligned} \quad (5.28)$$

The correlation C_2 is given by

$$\begin{aligned} C_2 &= N_2 - N_1 N_1 = \frac{1}{\sigma} \left(\frac{d\sigma^D}{dy_1 dy_2} + \frac{d\sigma^\pi}{dy_1 dy_2} \right) - \\ &\quad - \frac{1}{\sigma^2} \left(\frac{d\sigma^D}{dy_1} + \frac{d\sigma^\pi}{dy_1} \right) \left(\frac{d\sigma^D}{dy_2} + \frac{d\sigma^\pi}{dy_2} \right) \end{aligned}$$

or

$$\begin{aligned} C_2 &= \alpha N_2^D + (1-\alpha) N_2^\pi - (\alpha N_1^D(y_1) + (1-\alpha) N_1^\pi(y_1)) \times \\ &\quad \times (\alpha N_1^D(y_2) + (1-\alpha) N_1^\pi(y_2)) \end{aligned}$$

and finally:

$$\begin{aligned} C_2(y_1, y_2) &= \alpha C_2^D(y_1, y_2) + (1-\alpha) C_2^\pi(y_1, y_2) + \\ &\quad + \alpha(1-\alpha) (N_1^\pi(y_1) - N_1^D(y_1)) (N_1^\pi(y_2) - N_1^D(y_2)). \end{aligned} \quad (5.29)$$

Since diffractive processes are not supposed to populate the central region, C_2^D and N_1^D are negligible in that region; C_2^π corresponds to SRC and vanishes when $|y_1 - y_2|$ is large. Thus, for y_1 and y_2 in the central region and $|y_1 - y_2|$ large we have

$$C_2 \simeq \alpha(1-\alpha) N_1^\pi(y_1) N_1^\pi(y_2) \simeq \frac{\alpha}{1-\alpha} N_1(y_1) N_1(y_2). \quad (5.30)$$

The model is thus of the SRO kind, and integrating (5.30) one recovers the behaviour (5.26) of f_2 :

$$f_2 \simeq \frac{\alpha}{1-\alpha} \bar{n}^2 + O(\bar{n}).$$

The positive correlations observed in (5.30) are due to the fact that once a pion has been observed in the central region, this means that the event was of the pionization kind, and the probability of finding another pion in the central region is increased. The diffraction + pionization model realizes SRO in a very peculiar way, since all the constants a_k in (3.8) can be calculated in terms of one parameter only (see (5.27)).

One of the main virtues of DPM is that it makes the "true" correlation C_2^π much weaker than that which is displayed by the data. The argument I am going to present now is essentially that of Pirilä and Pokorski [31]. For the sake of definiteness I consider the $\pi^+ \pi^0$ correlations of the CHV experiment. The result of the experiment is given by the ratio

$$R(y_+, y_0) = \frac{C_2(y_+, y_0)}{N_1(y_+)N_1(y_0)}.$$

Hence

$$C_2^\pi(y_+, y_0) = \frac{1}{\alpha_\pi} \left(R(y_+, y_0) - \frac{\alpha}{1-\alpha} \right) a_+ a_0, \quad (5.31)$$

where a_+ and a_0 are the heights of the plateaux. In order to calculate $f_2^{\pi(+0)}$, I have to integrate C_2^π over y_+ and y_0 ; to get an estimate of the integral, I shall consider only the point $y_+ = 0$, and integrate over the domain where $R \geq \alpha/(1-\alpha) \simeq 0.3$:

$$f_2^{\pi(+0)} \simeq \frac{a_0 \bar{n}_+}{\alpha_\pi} \int_{R > \alpha_D/\alpha_\pi} \left(R - \frac{\alpha_D}{\alpha_\pi} \right) \Big|_{y_+=0} dy_0 = a_0 \bar{n}_+ I^{(+0)}. \quad (5.32)$$

The value found for $I^{(+0)}$ is ~ 0.6 . On the other hand, if we assume that the correlations are due to clustering, we have from (5.24):

$$\bar{n}_+^\pi = \bar{m} \bar{j}_+, \quad f_2^{\pi(+0)} = \bar{m} \bar{j}_+ \bar{j}_0. \quad (5.33)$$

Comparing (5.32) and (5.33) we get

$$I^{(+0)} \simeq \frac{\bar{j}_+ \bar{j}_0}{a_0 \bar{j}_+}. \quad (5.34)$$

If $\bar{j}_+ \bar{j}_0 \simeq \bar{j}_+ \bar{j}_0$, we find that the average number of π^+ 's (or π^0 's) per cluster is $a_0 I^{(+0)} \sim 0.6$. In the case of charged-charged correlations studied by Pirilä and Pokorski [31], (5.34) should be replaced by

$$I^c = \frac{\bar{j}(\bar{j}-1)}{a_c \bar{j}}. \quad (5.35)$$

Pirilä and Pokorski have taken a model of the diffractive component in order to evaluate more accurately the integral I^c in (5.32) (see Fig. 16). The model clearly reduces the amount of clustering which is necessary to reproduce the experimentally observed correlations. With short range correlations only, we would need 5–6 particles per cluster, while two are sufficient in DPM. In the latter case, one would expect the “true” $\pi^+ - \pi^+$ or $\pi^- - \pi^-$ correlations to be very weak, since the production of cluster with charge ± 2 seems unlikely.

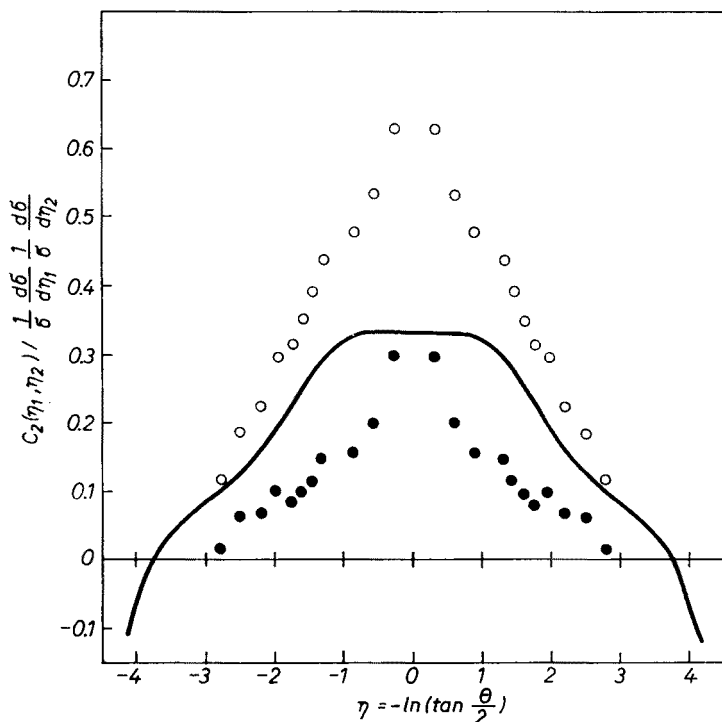


Fig. 16. Correlations from PSB experiment. Open points = experiment, full line = contribution from the diffractive and long range part. Full points: difference between the experimental correlation and the diffractive + “long range” part (Ref. [31])

Another interesting aspect of DPM is its possible relation with the inelastic proton spectrum for x near to 1. The inclusive cross-section for protons presents a peak for $x \geq 0.95$ in the ISR energy range, and this peak seems to be energy independent. The corresponding cross-section has been estimated to be ~ 7 mb [14], in agreement with previous estimates.

However, the fact that the peak scales shows that the missing mass M increases with s , since $M^2 \simeq s(1-x)$, while in the naive picture of diffraction one would expect something like

$$E \frac{d^3\sigma}{d^3p} \sim \frac{1}{\sqrt{s}} (1-x)^{-3/2}.$$

It seems possible that the picture of diffraction we have in mind is much too naive, and

it is obviously very important to investigate the properties of particles produced together with a proton having $x \geq 0.95$. In particular it would be very useful to know precisely what is the multiplicity associated with that peak, and how it varies with energy.

Another interesting possibility to investigate diffractive processes would be to measure semi-inclusive cross-sections $d\sigma_n/dy$ for small values of n : the naive diffraction picture predicts a two-bump structure, and it would be nice to know if it actually shows up. Finally it remains to give a better theoretical status to the model, since the incoherent superposition of two independent and disconnected mechanisms remains rather artificial and unsatisfactory.

6. Correlations between charged and neutral particles

To conclude this paper, I shall examine another kind of correlations, which seem to be interesting: the idea is to study the multiplicity distribution of one kind of particles, say b , while the number of another kind of particles, say a , is fixed in the final state. In practice one takes b to be neutral and a charged particles. Let me start again from the generating function

$$G(z_a, z_b) = \sum z_a^{n_a} z_b^{n_b} P(n_a, n_b). \quad (6.1)$$

I can calculate the factorial moment $F_k^b(n_a)$ as follows:

$$\begin{aligned} F_k^b(n_a) &= \overline{n_b(n_b-1) \dots (n_b-k+1) (n_a)} = \\ &= (P(n_a))^{-1} \sum_{n_b} n_b(n_b-1) \dots (n_b-k+1) P(n_a, n_b). \end{aligned} \quad (6.2)$$

It is then clear that $F_k^b(n_a)$ can be obtained by derivation of G at the point $z_a = 0$ (exclusive) and $z_b = 1$ (inclusive):

$$\begin{aligned} F_k^b(n_a) &= (P(n_a))^{-1} \frac{1}{n_a!} \frac{\partial^{n_a+k}}{\partial z_a^{n_a} \partial z_b^k} G(z_a, z_b) \Big|_{z_a=0}^{z_b=1} = \\ &= \frac{1}{\sigma_{n_a}} \int \frac{d\sigma_{n_a}}{dy_{b_1} \dots dy_{b_k}} dy_{b_1} \dots dy_{b_k}, \end{aligned} \quad (6.3)$$

where σ_{n_a} is the cross-section for producing n_a final particles and $d\sigma_{n_a}/dy_b$, for example, the semi-inclusive cross-section for measuring a particle b with rapidity y_b together with n_a particles in the final state.

Several models have been proposed in order to explain the experimental data on charged-neutral correlations. I shall now review the three most popular models, which are known as the σ , π and ϱ models [32].

σ -model

One assumes that pions are produced *via* isospin zero clusters which decay into two pions. The probability that such cluster decays into $\pi^+\pi^-$ ($\pi^0\pi^0$) is $p(q)$. From isospin

invariance, we must have, of course, $p = 2/3$, $q = 1/3$. Let $\tilde{G}(z)$ be the generating function for σ -production; we have from (5.23)

$$G(z_-, z_0) = \tilde{G}(pz_- + qz_0^2) \quad (6.4)$$

since $\lambda(z_-, z_0) = \sum w(n_-, n_0) z_-^{n_-} z_0^{n_0}$ and the only non-zero w 's are $w(1,0) = p$, $w(0,2) = q$. The z_0^2 term in (6.4) reflects the $\pi^0\text{-}\pi^0$ correlations coming from the $\pi^0\text{-}\pi^0$ decay mode. On the other hand there are no $\pi^-\pi^-$ correlations from the decay, and λ is linear in z . Because of these $\pi^0\text{-}\pi^0$ correlations, it is more convenient to work with the variable $l = 2n_0$; $\lambda(z_-, z_l) = pz_- + qz_l$. Let me first take the case where the σ 's are produced independently: $\tilde{G}(z)$ is then the generating function of a Poisson distribution:

$$\tilde{G}(z) = e^{\bar{N}(z-1)}, \quad (6.5)$$

where \bar{N} is the average number of σ 's. Then

$$\tilde{G}(z_-, z_l) = \exp \{ (pz_- + qz_l - 1) \bar{N} \} \quad (6.6)$$

and, taking derivatives at $z = z_l = 0$ we obtain

$$\begin{aligned} P(n_-, l) &= \frac{e^{-\bar{N}} (\bar{N})^N}{n_-! l!} p^{n_-} q^l = \frac{e^{-\bar{N}} (\bar{N})^N}{N!} \binom{n_- + l}{n_-} p^{n_-} q^l = \\ &= P(N) \binom{n_- + l}{n_-} p^{n_-} q^l, \end{aligned} \quad (6.7)$$

where $P(N)$ is the MD of σ . The repartition between the $\pi^+\pi^-$ and $\pi^0\pi^0$ decay modes is given by a binomial distribution.

In order to find the moments $F_k^l(n_-)$ we use (6.3)

$$F_k^l(n_-) = (P(n_-))^{-1} \frac{1}{n_-!} p^{n_-} q^k \tilde{G}^{(n_-+k)}(q)$$

while, from (2.30)

$$P(n_- + k) = \frac{1}{(n_- + k)!} p^{n_-+k} \tilde{G}^{(n_-+k)}(q).$$

Comparing both expressions we have [33]

$$F_k^l(n_-) = \frac{(n_- + k)!}{n_-!} \left(\frac{q}{p} \right)^k \frac{P(n_- + k)}{P(n_-)}. \quad (6.8)$$

In particular we have

$$F_1^0(n_-) = \overline{n_0(n_-)} = 2F_1^l(n_-) = \frac{(n_- + 1)P(n_- + 1)}{P(n_-)}. \quad (6.9)$$

Notice that if $P(n_-)$ is Poisson, then $\overline{n_0(n_-)}$ is independent of n : $\overline{n_0(n_-)} = \bar{n}_0$. From (6.9) we see that in the general case one can calculate $\overline{n_0(n_-)}$ from the experimental data on $P(n_-)$.

π -model

In the π model, one begins by assuming that each kind of pions follows a Poisson distribution:

$$P(n_+, n_0, n_-) = C(n_+, n_0, n_-) \frac{x^{n_+} x^{n_0} x^{n_-}}{n_+! n_-! n_0!}. \quad (6.10)$$

(Using the same x for n_+ , n_- , n_0 in (6.10) means that we shall have the same average number of π^+ , π^0 and π^- .) Now, charge conservation imposes that $n_+ = n_-$ so that

$$P(n_-, n_0) = \frac{e^{-x} x^{2n_-} x^{n_0}}{(n_-!)^2 n_0! I_0(2x)}, \quad (6.11)$$

where the Bessel function $I_0(2x)$ is there in order that the MD be normalized to one. This distribution has the following features: $\bar{n}_- \simeq \bar{n}_0 - 1/4$; it is narrower than Poisson for π^- 's: $f_2^- \simeq -\frac{1}{2} \bar{n}_-$; it is Poisson for π^0 's.

Now, as any MD can be written as a superposition of Poisson distributions, I can write the most general π -model as:

$$P(n_-, n_0) = \int_0^\infty f(x) dx \frac{x^{2n_-} x^{n_0} e^{-x}}{(n_-!)^2 n_0! I_0(2x)}. \quad (6.12)$$

From the trivial identity

$$\sum_{n_0} n_0(n_0-1) \dots (n_0-k+1) \frac{x^{n_0}}{n_0!} = x^k e^x$$

we immediately get

$$\sum_{n_0} n_0(n_0-1) \dots (n_0-k+1) P(n_-, n_0) = \int_0^\infty f(x) dx \frac{x^{2n_-+k}}{(n_-!)^2 I_0(2x)}$$

which is directly related to the charged MD $P(n_-+k/2)$. We thus have [33]

$$F_k^0(n_-) = \left(\frac{(n_-+k)!}{n_-!} \right)^2 \frac{P(n_-+k/2)}{P(n_-)} \quad (6.13)$$

and in particular

$$\overline{n_0(n_-)} \simeq \left(n_- + \frac{3}{4} \right) \frac{P(n_-+1/2)}{P(n_-)}. \quad (6.14)$$

 ϱ -model

In the ϱ model one produces ϱ^+ , ϱ^- and ϱ^0 which decay according to: $\varrho^+ \rightarrow \pi^+\pi^0$, $\varrho^- \rightarrow \pi^-\pi^0$, $\varrho^0 \rightarrow \pi^+\pi^-$. Let N_+ , N_- and N_0 be the number of ϱ 's; we have, assuming that the charge of the initial state is zero: $n_+ = N_+ + N_0$, $n_- = N_- + N_0$, $n_0 = N_+ + N_-$.

or

$$N_+ = N_- = l = n_0/2, N_0 = n_- - l. \quad (6.15)$$

Starting from a ρ MD analogous to (6.11):

$$P(N_-, N_0) = \frac{e^{-x} x^{2N_-} x^{N_0}}{I_0(2x) (N_-!)^2 N_0!} \quad (6.16)$$

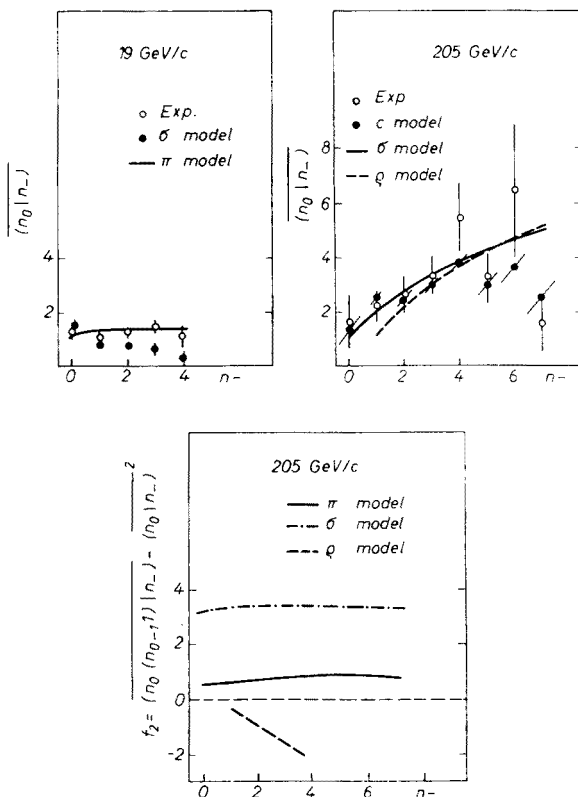


Fig. 17. $\overline{n_0(n_-)}$ and $f_2^0(n_-)$ calculated from the charged multiplicity distribution in the σ , π and ρ models (Ref. [33])

and substituting (6.15) we get

$$P(n_-, n_0) = \frac{e^{-x} x^{2l} x^{n_- - l}}{I_0(2x) (l!)^2 (n_- - l)!} \quad (6.17)$$

The results analogous to (6.8) and (6.13) in the case of the ρ -model are rather complicated, and I refer to the article by Drijard and Pokorski [33] for details.

The results for $\overline{n_0(n_-)}$ are compared with experimental data of Fig. [17]. One can see that the prediction of the σ -model are a bit too low, while those of the π and ρ models

are in agreement with experiment. The parameter $f_2^0(n_-) = F_2^0(n_-) - \overline{n^0(n_-)}^2$ calculated from the experimental charged MD is displayed on Fig. 17. One can see that the three models give rather different predictions, and it may turn out that experiment can discriminate between the various possibilities.

Approach from SRO

Another approach to the problem of charged-neutral correlations has been proposed recently by Krzywicki [6]. If the "Pomeron" exchanged in Mueller's theory has $I = 0$, and even if it is a very complicated singularity in angular momentum plane, one should have:

$$\overline{n_c^p n_0^q} \simeq \overline{n_c^{p+q}}, \quad (6.18)$$

since this $I = 0$ "Pomeron" does not distinguish between π^+ , π^0 and π^- . Then one should expect

$$\overline{n_c^p n_0^q} = c_{p,q} \overline{n_c^q} = c_{p+q} \overline{n_c^q} \quad (6.19)$$

which means that $c_{p,q}$ depends only on the sum $p+q$, and not on p and q individually. Krzywicki has indeed verified that $c_{p,1} = c_{p+1}$ within experimental errors at 205 and 303 GeV/c [6].

7. Conclusions

To conclude this paper, it seems fair to say that the short range order picture is in good qualitative agreement with experiment, at least for one and two-particle inclusive distributions and the multiplicity distribution. However, one may have to integrate over transverse momenta to get a valid picture. Further data, especially on $\pi^-\pi^-$ correlations, azimuthal correlations and MD at higher energies will be extremely useful in order to make further experimental verifications of this picture.

Finally, there are many interesting topics which have been omitted in this paper: for example the correlations between particles produced together with a leading proton, the correlations associated with large transverse momenta, and certainly many other kinds of correlations I have not been able to think of.

REFERENCES

The literature on inclusive reactions in general and on correlations in particular is so large that I cannot give a complete list of references, and the following list is rather arbitrary. For a more complete bibliography, see for example the review papers of Jacob at the NAL Conference, or of Koba at the 1972 Zakopane meeting.

- [1] K. Wilson, *Acta Phys. Austriaca*, **17**, 37 (1963).
- [2] R. Feynman, *Phys. Rev. Letters*, **23**, 1415 (1969).
- [3] J. Benecke, T. T. Chou, C. N. Yang, E. Yen, *Phys. Rev.*, **188**, 2159 (1970).
- [4] K. Gottfried, *CERN lecture notes*, TH 1615 (1973).
- [5] A. Mueller, *Phys. Rev.*, **D4**, 150 (1971).

- [6] The concept of short range order was first discussed in these terms by A. Krzywicki, *CERN preprint* TH 1633 (1973).
- [7] M. Le Bellac, *Phys. Letters*, **37B**, 413 (1971). The proof which is given in the text is inspired by that of L. Brown, *Phys. Rev.*, **D5**, 748 (1972).
- [8] M. Le Bellac, *Nuovo Cimento Letters*, **2**, 437 (1971); H. Harari, *Phys. Rev. Letters*, (1973).
- [9] L. Caneschi, *Proceedings of the VII Moriond Rencontre* (1972).
- [10] D. Sivers, G. Thomas, *Phys. Rev.*, **D6**, 1961 (1972).
- [11] E. Berger, B. Oh, G. Smith, *Phys. Rev. Letters*, **29**, 675 (1972).
- [12] J. Beaupré *et al.*, *Phys. Letters*, **40B**, 510 (1972).
- [13] CERN-Hamburg-Vienna collaboration, *CERN preprint*, to be published in *Phys. Letters B* (1973).
- [14] J. C. Sens, *Invited paper presented at the Conference on recent advances in particle physics* (1973).
- [15] See for example A. Bassetto, L. Sertorio, M. Toller, *Nuclear Phys.*, **B34**, 1 (1971).
- [16] 50 and 69 GeV/c: Soviet-French collaboration, *Phys. Letters*, **42B**, 519 (1972);
102 GeV/c: J. Chapman *et al.*, *Phys. Rev. Letters*, **29**, 1686 (1972);
205 GeV/c: G. Charlton *et al.*, *Phys. Rev. Letters*, **29**, 515 (1972);
303 GeV/c: F. Dao *et al.*, *Phys. Rev. Letters*, **29**, 1627 (1972).
- [17] Bucharest-Budapest-Cracow-Dubna-Hanoi-Serpukhov-Sofia-Tashkent-Tbilisi-Ulan Bator-Warsaw collaboration, *Warsaw preprint* (1972); IPHE-Mons-Saclay collaboration, presented at the NAL Conference (1972).
- [18] O. Czyżewski, K. Rybicki, *Nuclear Phys.*, **B47**, 633 (1973); A. Wróblewski, *Warsaw preprint* 7212 (1972).
- [19] P. Slattey, *Rochester preprint* (1972).
- [20] Z. Koba, H. Nielson, P. Olesen, *Nuclear Phys.*, **B40**, 317 (1972).
- [21] M. Le Bellac, J. L. Meunier, G. Plaut, *Nuclear Phys.*, to be published (1973).
- [22] The following proof of KNO scaling was suggested to me by J. L. Meunier.
- [23] H. Weisberg, *University of Pennsylvania preprint* (1973); See also A. Buras, Z. Koba, Niels Bohr *preprint* 73-1 (1973).
- [24] D. Weingarten, Niels Bohr *preprint* 73-5 (1973). I wish to thank F. Guerin for an illuminating presentation of the ideas contained in this paper.
- [25] Z. Koba, D. Weingarten, Niels Bohr *preprint* 73-10 (1973).
- [26] W. Weisberger, *Stony Brook preprint* (1973).
- [27] K. Wilson, *Cornell University preprint* (1970).
- [28] A. Białas, K. Fiałkowski, K. Zalewski, *Nuclear Phys. B* (1973); K. Fiałkowski, *Phys. Letters*, **41B**, 379 (1972); K. Fiałkowski, H. Miettinen, *Phys. Letters*, **43B**, 61 (1973).
- [29] W. Frazer, R. Peccei, S. Pinsky, C. I. Tan, *UCSD preprint*, to be published in *Phys. Rev. D* (1973).
- [30] H. Harari, E. Rabinovici, *Phys. Letters*, **43B**, 49 (1973).
- [31] P. Pirilä, S. Pokorski, *Phys. Letters*, **B43**, 502 (1973).
- [32] E. Berger, D. Horn, G. Thomas, *ANL preprint*, to be published in *Phys. Rev. D* (1973).
- [33] D. Drijard, S. Pokorski, *Phys. Letters*, **43B**, 509 (1973).